Applied Energy 347 (2023) 121410

Contents lists available at ScienceDirect

Applied Energy

journal homepage: www.elsevier.com/locate/apenergy

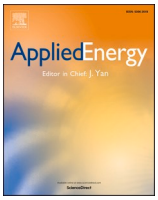

Design of sustainable offshore hybrid energy systems for improved wave energy dispatchability

Mariasole Cipolletta, Anna Crivellari, Valeria Casson Moreno, Valerio Cozzani *

Laboratory of Industrial Safety and Environmental Sustainability - DICAM, University of Bologna, Via Terracini 28, Bologna 40131, Italy

HIGHLIGHTS

- A methodology for sustainable design of offshore hybrid energy systems is developed.
- Wave energy dispatchability issues are considered.
- Stranded gas in end-of-life reservoirs may be used to foster energy transition.
- Wave energy exploitation enhanced by offshore stranded gas-based back-up systems.
- Test cases in the North Sea and Adriatic Sea were carried out.

ARTICLE INFO

Keywords:
Offshore hybrid energy systems
Sustainable design
Offshore renewable energy sources
Wave energy
Grid integration

ABSTRACT

Wave energy is a renewable energy source having a highly exploitable potential in several locations worldwide. In the framework of energy transition, the exploitation of wave energy combined with end-of-life offshore stranded gas reservoirs may lead to two positive impacts: the stabilization of the energy supplied to the grid and a better penetration of renewable energy in areas where the grid is not able to compensate the fluctuations associated to renewable energy production. Moreover, in order to guarantee the dispatched energy schedule, wave energy needs to be coupled with back-up systems aimed at valley filling. In the present study, an innovative approach to the conceptual design of hybrid energy systems based on wave energy is developed, entailing an operation strategy that complies with the dispatching needs of grid-connected generation systems. The probability of correct dispatching that the producer assures to the Transmission System Operator is used as a parameter to optimize the design of a Gas to Power back-up system used for valley filling. The approach supports the preliminary design of offshore hybrid energy systems based on wave energy, starting from historical wave data up to the definition of an optimal back-up system valorizing residual reservoir fuels and its operation strategy. The proposed design is evaluated through a Multi-Criteria Decision Analysis, including the technological, economic, environmental and safety aspects, which allows the assessment of the overall sustainability performance of the hybrid system, considering the fluctuations associated to wave power generation during a typical operation period. The methodology was applied to two test-cases in different offshore operating theaters (North and Adriatic seas), in order to test its potentiality. The results highlighted that, in both sites, similar design choices are suggested for the hybrid system. However, the annual energy production resulted 6.5 times higher in the North Sea test-case. The low energy generation in the Adriatic Sea test site caused a levelized cost of energy of 3960 EUR/MWh, much higher than the value obtained for the North Sea case (610 EUR/MWh). In both cases, the gas turbine park impacts negatively on the cost of energy production, but is critical in meeting the design value of the probability of correct dispatching.

1. Introduction

In recent years, uncountable efforts were made to efficiently and profitably exploit Renewable Energy Sources (RESs). In 2019, 11.6% of primary energy and 26.7% of worldwide generated electricity were obtained from these unlimited sources [1]. The sharp increase in renewable energy generation after 2001 [2], supported by public

* Corresponding author.
E-mail address: valerio.cozzani@unibo.it (V. Cozzani).

https://doi.org/10.1016/j.apenergy.2023.121410
Received 30 December 2022; Received in revised form 1 March 2023; Accepted 6 June 2023
Available online 25 June 2023

Nomenclature

List of Acronyms

AEP	Annual Energy Production
AHP	Analytic Hierarchy Process
ASI	Aggregated Sustainability Index
CAPEX	CAPital Expenditures
CDF	Cumulative Distribution Function
EFLH	Equivalent Full Load Hours
G2P	Gas To Power
GHG	Greenhouse Gas
GT(s)	Gas Turbine(s)
GTP	Gas Turbine Park
HVAC	High Voltage Alternating Current (HVAC)
KPI(s)	Key Performance Indicator(s)
LCOE	Levelized Cost Of Energy
LEE	Levelized Energy Efficiency
LGHG	Levelized Greenhouse Gases emissions
LHI	Levelized inherent Hazard Index
LVOE	Levelized Value Of Energy
MCDA	Multi-Criteria Decision Analysis
NG	Natural Gas
OPEX	OPerative Expenditures
PTO	Power-take-off
RE(s)	Renewable energy(ies)
RES(s)	Renewable energy source(s)
TSO	Transmission System Operator
WD	Wave Dragon
WEC(s)	Wave Energy Converter(s)
WF(s)	Wave Farm(s)

investments in the sector [3], is due to the growing awareness that the worldwide exploitation of RESs is a key requirement considering several issues: the unequal distribution of fossil resources, their depletion, and, mostly, the effects of climate changes caused by Greenhouse Gas (GHG) emissions. These factors, however, strongly claim the need for an even higher penetration of cleaner energy sources and for the development of more efficient systems for RESs exploitation in production and transformation processes [4]. Thus, the widespread and improved use of Renewable Energy (RE) can make great strides towards the sustainability of anthropic activities from the social, economic and environmental perspectives.

To this purpose, seas and oceans are unlimited sources of wave energy, tidal energy, currents, salinity gradients and ocean thermal energy, scoring a total theoretical potential up to 114,000 TWh/y of RE, whose exploitation would exceed the global electricity demand by 400% [5]. Moreover, 95% of countries worldwide are bathed by seawater [6]. Yet, the exploitation of such energy potential is still limited: the International Energy Agency highlighted that ocean energy generation is not on track with the targets foreseen for 2025 and 2030 (4 and 15 TWh, respectively) set by the European Commission [7]. Several studies addressing the strategies for producing and delivering offshore renewable energy are available in the literature, assessing the relevance of different energy vectors [8]. In recent years there was a fast development of Wave Energy Converters (WECs) [9], exploring a variety of hydrodynamic and generation principles [10] as well as looking at several possible applications, such as built-in ocean observing platforms [11] and autonomous underwater vehicles [12]. Nevertheless, the very specific design, the demanding installation and operation procedures and the uncertainty in the actual RE delivered to the shore still result in a high Levelized Cost of Energy (LCOE) (0.30 – 0.55 USD/kWh) with respect to other RESs conversion technologies [13]. As a consequence, hybrid systems are often considered a viable and convenient option for the valorization of wave energy since the combination of different offshore energy sources may avoid the presented bottlenecks: Hu et al. (2020) approach the design of a floating wind farm supporting WECs through a numerical study that enables the optimization of the number and configuration of the converters [14]; Kluger et al. (2023) evidenced the power balancing effects deriving from wind-wave hybrid systems [15].

As in the case of other RESs, the profitable exploitation of wave energy depends on the capability to accurately characterize the wave features, in order to perform the optimized design of the energy harvesting devices. For instance, despite several research efforts in this field, Jiang et al. (2022) highlighted that seldom wave characteristics are derived by accounting for the different wave systems composing the wave field [16]. Additionally, Coe et al. (2021) highlighted that the wave resource information is often wrongly accounted in WECs design, being the RES intermittency and the device capacity factors too often neglected, thus leading to the overestimation of the potentialities of locations with a high average wave resource power [17]. Also, wave energy is challenged by its aleatory variability, since marine and meteo-climatic conditions determine the real-time output of WECs [18].

In order to face the variability of power production from RESs, the Transmission System Operator (TSO) requires the company operating the RESs converters to define in advance a daily dispatching power plan [19]. To reduce the risk related to the randomness of RESs and to foster the improvement of the dispatching forecast, a common principle is to impose to the energy suppliers a probability of correct dispatching (i.e. to correctly produce the scheduled power), thus penalizing them when the produced power diverges for an error higher than the allowable one (calculated with respect to the forecast). In addition, when the installed capacity of renewable systems is higher than 5 MW, simulation data of the dynamic transients have to be provided, since the grid core requirements have to be strictly respected for the stability and operation of the grid itself [20].

Short-term forecasting is frequently used to balance generation and load in the case of RESs exploitation, and shows better predictability for wave than for solar and wind energy [21]. Even so, uncertainty affects the actual possibility of complying with the dispatching plan. This issue can be overcome by fossil fuel-based back-up systems able to respond to renewable power shortages, applying the so-called valley filling technique [22]. Gas turbines (GTs) are the generation systems most widely applied to this purpose, due to their compactness, the short time required for their start-up and the wide declination of sizes [23]. Moreover, Du Toit et al. (2020) evidenced the flexibility of Natural Gas (NG) microturbines towards co-combustion of fuel mixtures containing CO_2 and H_2, in the perspective of off-grid and emergency back-up of power applications [24]. In offshore, specific benefits may derive from synergies with fossil fuel exploitation and/or the decommissioning of depleted gas fields [25]. Actually, the decommissioning of hydrocarbon fields is usually not started after the complete depletion of the reservoir, but rather at the break-even point for economic benefits considering the progressive reduction in the well pressure and/or in the quality of the extracted fossil resources, that causes increasing costs in the resource delivery to the shore [26]. Thus, depleted oil&gas fields facing decommissioning are often not completely exploited, while the associated infrastructure is still operable and the stranded gas is available on site, representing a possible fuel for a back-up system and for Gas To Power (G2P) applications [25].

Several studies addressing the coupling of wave farms (WFs) with G2P systems are available in the literature. Ou et al. (2017) demonstrated the application of a novel damping controller for the static synchronous compensator in a hybrid power system made of an offshore wind farm, a seashore wave farm, a battery storage system and a microturbine park [27]. Oliveira-Pinto et al. (2019) explored the niche

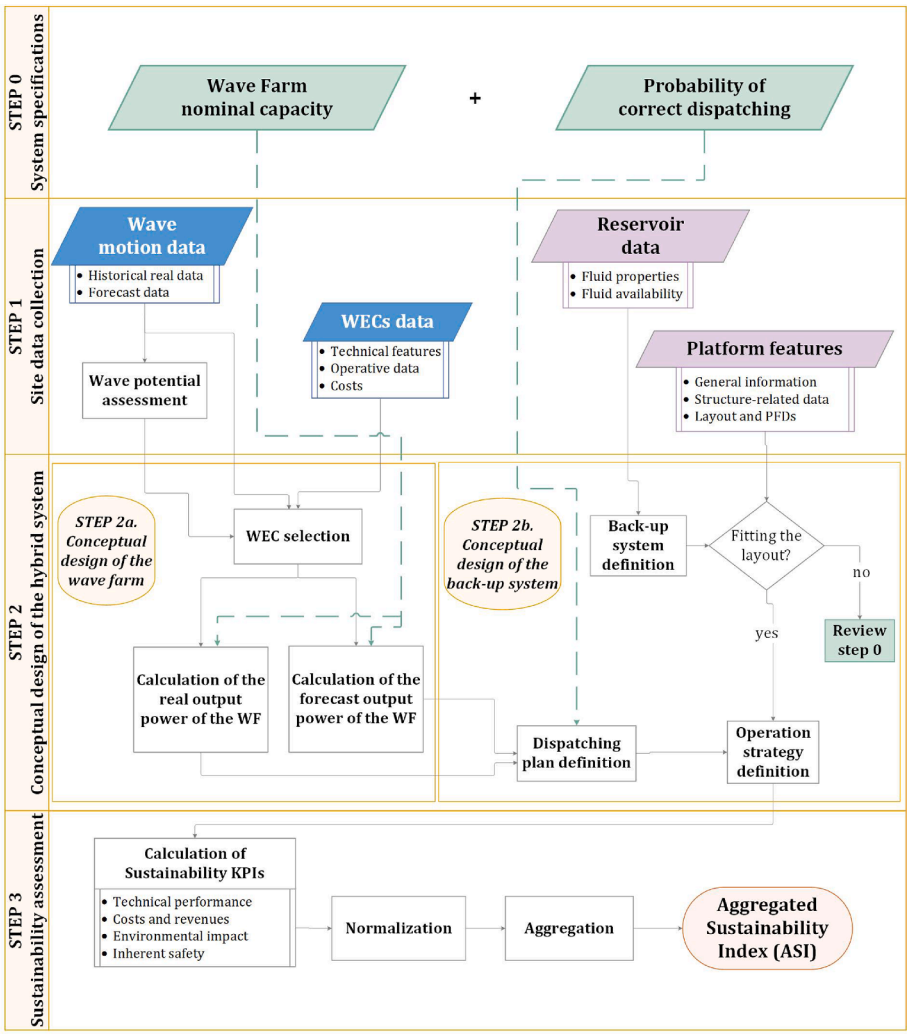

Fig. 1. Flow chart of the methodology developed for the conceptual design of offshore hybrid energy systems based on wave energy and G2P.

market of wave energy power generation for the power supply to an oil and gas production platform in the Norwegian Continental Shelf, by halving the capacity of the existent gas turbine park [28]. G2P was also selected as the suitable back-up strategy for a desalination facility mainly powered by wave and solar energy on the island of Tenerife [29]. Recently, Dincer et al. (2021) proposed the design of offshore hybrid energy systems based on Multi-Criteria Decision Analysis (MCDA), specifically addressing G2P applications to support wind energy harvesting [30].

In the work of Nasrollahi et al. (2023), a comprehensive review of WEC assessment methods and MCDA tools is reported. The authors also report the application of different assessment criteria to a set of WECs proposed for industrial scale-up [31]. The proposed prioritization approach, entailing both the Fuzzy Delphi and the PROMETHEE methods, is demonstrated through an application to the Caspian Sea, whose wave energy potential was confirmed by the results of extensive numerical simulations carried out by Jahangir et al. [32].

In this framework, the present study aims at the development of an innovative methodology for the conceptual design of sustainable hybrid energy systems based on wave energy, using offshore G2P systems as a back-up for valley filling. The main novelty of the methodology consists in the inclusion of the constraints deriving from the preparation of an optimal dispatching plan in the conceptual design of these novel systems, in order to comply with a stabilized power supply to the grid. Indeed, the influence of the dispatching plan on the design of a generation system was seldom considered in previous studies, even if it plays an important role on the overall sustainability of non-programmable RESs exploitation, in particular with respect to technical and economic constraints. Therefore, in the present study, the dispatchability of the energy produced was assumed as a main factor in the design and operation of a hybrid system. Moreover, the method developed provides a set of Key Performance Indicators (KPIs) addressing the performance in the different sustainability domains (economic, environmental and social) of the hybrid systems under design, in addition to those addressing the technological performance. The methodology is especially valuable in the comparison of alternative sites considered for wave energy exploitation. Actually, the MCDA approach developed enables the conceptual design optimization and the assessment of the broad sustainability of technological alternatives considered for RESs exploitation in each site.

Two test cases were analyzed, one in the North Sea and the other in the Adriatic Sea, in order to explore the potentiality of the methodology and to assess the influence of site-specific parameters on the hybrid system design and on its sustainability performance.

In the following, section 2 presents the proposed methodology. In section 3, the test cases are described. Section 4 presents and discusses the main results of the test cases, while conclusions are reported in section 5.

2. Methodology

A methodology supporting the conceptual design of offshore hybrid

Table 1
Site-specific input data collected in step 1 of the methodology.

Wave motion
a. Wave periods (T_m, T_p)
b. Significant wave height (H_s)
c. Wave direction (θ)
WEC
a. Technical features: sizes, installation requirements
b. Operative data: ranges and performance curves
c. CAPEX and OPEX
Reservoir
a. Reservoir fluid properties: composition, heating value
b. Reservoir fluid availability: residual pressure, flow rate
Offshore platform
a. General information: type, remaining lifetime
b. Structure-related data: size, elevation of decks
c. Layout of actual equipment and process flow diagrams (if possible)

systems exploiting wave energy was developed, entailing the preparation of an operation strategy that complies with the dispatching needs of grid-connected generation systems.

Fig. 1 shows the main steps of the methodology. The procedure initially requires the definition of the parameters needed for the hybrid system specification: the nominal capacity of the WF (P_{WF}) to be installed and the probability of correct dispatching ($Prob_d$) that the producer commits to deliver to the TSO (step 0 of Fig. 1: System specifications).

Step 1 consists in the collection and analysis of data related to the selected site(s) in a reference period. Step 2 foresees the design of the hybrid system, starting from the WF (step 2a). On the basis of historical real and forecast data, a dispatching plan is then obtained, driving the optimal selection and sizing of the back-up system (step 2b).

In case alternative sites are considered for the installation of the hybrid generation system, a further step based on MCDA is proposed for the assessment and comparison of the sustainability performance of each alternative.

2.1. Data collection

In step 1 of the methodology, the site-specific data needed for the conceptual design of the hybrid system are gathered. Table 1 summarizes the data that need to be collected.

Meteo-climatic parameters describing the wave motion are collected over a reference period of at least 1 year with a minimum time resolution of 1 h, as to study seasonality and to comply with the energy market pricing methods [33]. The required data are: the significant wave height H_s [m], the mean wave period T_m [s], the peak wave period T_p [s] and the wave direction θ [-] [29]. In alternative to rough data directly obtained from real-time measurements, aggregated data from long-term trend analysis may also be used [34]. Starting from these parameters, the quantification of the wave potential is carried out to allow the WEC selection (step 2a). The wave potential is quantified calculating $P_{w,av}$ [W/m], the average of the hourly wave energy flow $P_{w,t}$ [W/m] throughout the reference period. $P_{w,t}$ represents the power per unit of surface of the crest length at the t-th hour and may be estimated as follows [19]:

$$P_{w,t} = \frac{1}{64\pi} \bullet \rho_{water} \bullet a_g{}^2 \bullet H_{s,t}^2 \bullet T_{m,t} \quad (1)$$

where ρ_{water} is the seawater density (1025 kg/m^3) and a_g [m/s^2] is the gravitational acceleration constant. Forecast data of the same wave parameters with a time horizon of 6 h [35] and referring to the same reference period also need to be retrieved. An in-depth discussion of real and forecast data types and analysis is reported in section A1 of Appendix A.

WEC data also need to be collected in step 1 of the methodology. Data about the available WECs technologies are gathered from dedicated literature and from the available technical sheets. The selection of the proper WEC starts by considering the relevant site specific data (water depth and distance from shore). The technological readiness level and the operative ranges of the device are also relevant, requiring the selection of technologies demonstrated on the full scale in conditions similar to those of the site of interest. The set of suitable devices selected by this procedure is the input to Step 2, where the specific device used in the design will be selected considering the power generation performance.

Information concerning the reservoir fluid and its availability, as well as the features of the offshore platform, also need to be collected in step 1 in order to carry out the conceptual design of the back-up system in the following steps of the procedure.

2.2. Conceptual design of the hybrid power system

As shown in Fig. 1, the preliminary design of the hybrid system (step 2) is divided in two parts: step 2a aims at the conceptual design of the WF, while step 2b addresses the back-up system design.

2.2.1. Conceptual design of the wave farm (step 2a)

First, the WEC technology to be used has to be selected. The selection is carried out through the comparison of the generation performances of the devices which were identified in step 1 as suitable to exploit the $P_{w,av}$ previously calculated. In detail, the hourly power generation curve $P_{WEC}(t)$ [MW] in the t-th hour needs to be calculated for each device. The modelling approach proposed by [36] was used in the present study. It consists in the calculation of the WEC absorbed power by the use of the WEC specific power matrix and in its correction considering power-take-off (PTO) and generator efficiencies:

$$P_{WEC}(\mathrm{t}) = P_{w,abs}(\mathrm{t}) \bullet \eta_{PTO} \bullet \eta_{gen} \quad (2)$$

$P_{w,abs}(\mathrm{t})$[MW] is the power absorbed by the device. The parameters η_{PTO} [-] and η_{gen} [-] are respectively the PTO and the generator efficiencies, whose values depend on the specific type of PTO and electric generator used [36].

The power absorbed by the device, $P_{w,abs}(\mathrm{t})$, is calculated applying the specific WEC power matrix to the meteo-climatic parameters (bins (H_s, T_m) or (H_s, T_p)) occurring in the t-th hour [37]. The power matrix of a WEC is specified by the manufacturer and provides the WEC power output for all operative combinations of wave height and wave period ((H_s, T_m) or (H_s, T_p)) in the wave direction operative range (θ_{min} - θ_{max}) of the WEC.

The good practice suggests to consider the possibility of adaptation of the device size to make the most of the specific meteo-climatic conditions, taking into account that WECs are site-specific and scalable devices [36]. The theoretical principles on which WECs are scaled are reported in the literature [38]. Details on the theory of wave generators and a summary of the scale parameters used in the present study are reported in section A2 of Appendix A.

Finally, it should be mentioned that the developed approach is limited to the conceptual design of the WF. Thus, the proposed design does not address the lay-out of the WECs in the WF, neither its effects on the expected power output of the WF.

Once the power output of each WEC is obtained, the Annual Energy Production (AEP_{WEC}) [MWh] is evaluated with Eq. (3):

$$AEP_{WEC} = AV_{WEC} \bullet \sum_{t=1}^{m} P_{WEC}(t) \quad (3)$$

where m [h] is the number of hours in the reference period (8760 in a year), AV_{WEC} [-] is the WEC availability (i.e., the time fraction during which the device is available to produce power excluding any operation

and maintenance intervention). A value of 0.90 was assumed for AV_{WEC}, as suggested in the literature [39].

The most suitable WEC for the site is identified according to the following performance indicators, which were selected due to their relevance in determining the technological performance of the devices:

- AEP_{WEC}, as defined in Eq. (3): the yearly energy generation of the device in cumulative terms, independently of the time trend of the power output;
- $\overline{P}_{WEC}$[MW]: the average power produced by the device in the reference period, indicating if the renewable plant is able to provide a defined design load;
- *CF*, the Capacity Factor [-] [40]: this parameter quantifies the ratio between $\overline{P}_{WEC}$ and the nominal power of the device ($P_{WEC,nom}$), providing the average operation level of the device within the boundaries of its own capacity. Thus, *CF* is a critical indicator of technological performance, also allowing a comparison with the efficiencies of other renewable energy converters;
- *CW*, the Capture Width [m] [40], i.e. the ratio between $\overline{P}_{WEC}$ and the wave potential $P_{w,av}$: this parameter allows the comparison of the overall power generation of the WEC device with respect to the average potential of the wave resource in the site considered for installation. Actually, the indicator expresses the equivalent wave length that the WEC is able to absorb and to convert at a given site.

Clearly enough, a higher value of each parameter corresponds to a higher performance of the WEC device. Thus, in order to select the most performing WEC, the device scoring the overall highest performance based on the above-listed parameters should be selected. To this purpose, a straightforward multi-objective approach is applied. The approach is divided into two steps: the internal normalization and the calculation of the average of the normalized indicators. A linear internal normalization is adopted in the range [I_{min}, I_{max}] according to the equations presented in section A4 of Appendix A. I_{min} and I_{max} are defined as the lowest and the highest figures obtained for each criterion considered in the MCDA within the compared WECs. In order to rank the overall performance of each device, the values of the normalized indicators are summed and divided by four. The WEC device scoring the highest performance index is selected for application.

The required number of WECs (N_{WECs}) is then calculated, considering the design WF capacity P_{WF}.

The real output power of the WF, P_r, is obtained by multiplying P_{WEC} by N_{WECs}. In this approach, the power supplied to the grid is assumed to be the gross power produced by the WF, neglecting inter-array losses related to wake effects and electrical losses deriving from inter-array cables, export cables and the High Voltage Alternating Current (HVAC) substation [41]. This assumption is suggested in the literature for HVAC cables operating at a maximum rating of 200 MW and 150–170 kV. Such systems are used for small distances between the offshore site and the onshore grid delivery point (i.e. 20–50 km), as in the case of G2P offshore hybrid energy solutions [42].

Similarly, P_f, the forecast output power of the WF, is obtained by applying Eq. (2) to the forecast meteo-climatic data, multiplying the result by the required number of WECs, N_{WECs}.

2.2.2. Conceptual design of the gas turbine park (step 2b)

This step is aimed at defining the type, the nominal power and the total number of the machines to be installed in the gas turbine park (GTP) of the hybrid generation system. An innovative procedure, applying the method of dispatching errors proposed by Dincer et al. [30] was used.

In the definition of the dispatching plan, power prediction errors are calculated as in Eq. (4), where $\xi(t)$ [kW] is the hourly absolute error between the real and forecast output powers of the WF.

$$\xi(t) = P_r(t) - P_f(t) \tag{4}$$

As a matter of fact, $\xi(t)$ has a negative value if the energy generated and supplied to the grid is lower than the planned value. If the energy generated is higher than the forecasted value, a positive value is obtained.

Once estimated, the errors, $\xi(t)$, are statistically analyzed over the time intervals I_i considered for the reference period (i.e., one-month intervals in a reference period of one year, therefore i = 12). Then, the error distribution is fitted applying a best-fitting model based on accuracy criteria. Herein, the Anderson-Darling fitting model was considered due to both its suitability in comparing different series and its adaptability to data tails. Subsequently, the probability density function and the cumulative distribution function (CDF) of the samples are obtained.

As stated earlier, in the definition of the dispatching plan, a given value of $Prob_d$ (lower than 100%) was assumed: i.e. a $Prob_d$ of 80% implies assuming that in the 20% of the time the RES exploited is not sufficient to produce the forecast power [43]. Based on this probability value, the absolute dispatch error $\xi_d(i)$ per each time interval is calculated. The prediction error corresponding to the CDF of probability of incorrect dispatching equal to the complement of $Prob_d$ in the i-th time interval $N_\xi(i)$ is indicated as $\xi_d(i)$ and may be calculated as follows:

$$\xi_d(i) = \xi : N_\xi(i) = 1 - Prob_d \tag{5}$$

As an example, if $Prob_d$ is 80% and 12 months are analyzed, 12 allowable $\xi_d(i)$ are calculated which correspond to a cumulative probability of incorrect dispatching of 20% (i.e. $N_\xi(i) = 20\%$).

Finally, the hourly dispatched power $P_d(t)$ can be obtained from $P_f(t)$ considering the absolute dispatch error $\xi_d(i)$ [kW] for each time interval:

$$In\ each\ I_i: \ P_{d,i}(t) = P_{f,i}(t) - \xi_d(i) \tag{6}$$

Therefore, the $P_d(t)$ declared for grid injection needs to be lower than the hourly forecast power $P_f(t)$ to avoid or at least to reduce prediction errors as much as possible. Thus, once defined the dispatching plan, the conceptual design of the GTP may be carried out (step 2b). The necessary back-up power from the GTP (P_{GTP}) is defined considering the maximum power that should be provided by the turbo machines, $P_{GT}(t)$ assuming $Prob_d$ equal to 100% (i.e., P_f equal to P_d at each hour):

$$P_{GTP} = max_t(P_{GT}(t)) \tag{7}$$

The equipment model selection is then carried out, taking into account the nominal power and the footprint of the single machines. Among the available GT models, compact and light-weight aero-derivative GTs are suitable for power generation at offshore platforms in the low-medium range (4–66 MW), while micro-GTs are usually the best option for smaller capacities (<1 MW). After the selection, the nominal power at full load ($P_{GT,nom}$), the nominal efficiency at full load ($\eta_{GT,nom}$) and the size of the machine are noted. The total number of GTs (N_{GT}) needed to obtain the P_{GTP} is calculated considering their nominal capacity.

The total footprint of the GTs is also assessed. The footprint needed for GT installation needs to be compared with the available free space of the decks of the offshore structure. In case the footprint of the back-up system exceeds the free space available on the decks of the offshore platform, the system specifications have to be revised.

The GTP is assumed to be operated according to the approach suggested by Guandalini et al. (2015) [43]. Thus, on the basis of the declared $P_d(t)$, the GTP guarantees a flexible and efficient power provision through the intelligent operation of the turbines in parallel and at the same part-load. Further details on the calculation of the part-load efficiency of low-medium and micro-GTs are reported in section A3 of Appendix A. The hourly power provided by the back-up fuel is obtained as the ratio of P_{GT} to η_{GT}. The related fuel consumption and emissions are then quantified and used in the sustainability assessment.

Table 2
Reference values assumed for the normalization of the five sustainability indicators.

Key Performance Indicator	Definition	Reference Equation	Sustainability domain		Reference boundary	Description	Source
LEE[%]	Energy efficiency of the hybrid system in the analyzed period	Eq. (8)	**Technological**	I_{min}	0	Worst case efficiency (no energy production)	—
				I_{max}	78	Highest performance from overtopping WECs	[50]
LCOE[EUR/MWh]	Distributed production costs of produced energy from the hybrid system over its lifetime	Eq. (11)	**Economic**	I_{min}	210	Minimum LCOE for overtopping WECs	[36]
				I_{max}	664	Maximum LCOE for overtopping WECs	[36]
LVOE[EUR/MWh]	Distributed revenues from the sale of produced energy from the hybrid system over the analyzed period	Eq. (12)	**Economic**	I_{min}	0	Minimum recorded incentive on marine energy	[51]
				I_{max}	582	Maximum recorded incentive on marine energy (Portugal, 2006)	[51]
LGHG[ton_{CO2eq}/MWh]	Levelized GHG emissions from the hybrid system over the analyzed period	Eq. (13)	**Environmental**	I_{min}	0	Less polluting EU country in 2018 (Norway)	[52]
				I_{max}	0.9	More polluting EU country in 2018 (Estonia)	[52]
LHI[m^2/y]	Levelized Inherent hazard risk from the operation of the hybrid system over the analyzed period	Eq. (14)	**Societal**	I_{min}	0	No GT operating	—
				I_{max}	0.18	GTP at regime coupled with NG extraction offshore platform operation	[46]

2.3. Sustainability Key performance indicators

In step 3 of the methodology (see Fig. 1), KPIs related to the sustainability performance of the hybrid system are calculated. The KPIs aim at scoring the sustainability performance of the hybrid generation system designed in step 2. Therefore, the KPIs may be used as drivers to select among alternative siting options, as well as to identify the most sustainable design options and/or to identify critical issues in the outcome of conceptual design obtained from step 2.

A total of five KPIs are defined, addressing the different pillars of sustainability, as summarized in Table 2. As shown in the table, an innovative feature of the present study is the introduction of specific indicators to assess the expected safety performance of the hybrid system [30]. The approach entails the use of inherent safety indicators that proved effective in a large variety of applications, addressing both conventional [44] and innovative processes for energy vectors production, onshore [45] and offshore [46]. In the following, the procedure for the calculation of each KPI is described.

A novel indicator, the Levelized Energy Efficiency (*LEE*), is defined to assess the WF performance in the selected site, given that the GTP always runs at the highest possible efficiency. The *LEE* [-] weighs the contributions of the WF and the GTP energy conversion efficiencies over the m [h] hours of the reference period:

$$LEE = \frac{\eta_{WF,av} h_{WF} + \eta_{GTP,av} h_{GTP}}{m} \tag{8}$$

where $\eta_{WF,av}$ [-] and $\eta_{GTP,av}$ [-] are the average energy conversion efficiencies of the offshore WF and of the GTP during their respective operation periods, h_{WF} [h] and h_{GTP} [h].

The values of $\eta_{WF,av}$ and $\eta_{GTP,av}$ are the averages of the hourly efficiencies $\eta_{WF,t}$ [-] and $\eta_{GTP,t}$ [-], over their operative periods, defined as follows:

$$\eta_{WF,t} = \frac{P_{WF,t}}{P_{w,t} L_{char}} \tag{9}$$

$$\eta_{GTP,t} = \frac{P_{GTP,t}}{P_{GT,nom} N_{GT,t}} \tag{10}$$

where $P_{WF,t}$ [MW] is the real power produced by the WF in the t-th hour and L_{char} [m] is the characteristic length of the WEC. Similarly, $P_{GTP,t}$ [MW] is the GTP power output in the t-th hour, $P_{GT,nom}$ [MW] is the nominal capacity of a single turbine, and $N_{GT,t}$ [-] refers to the number of turbines activated in the t-th hour.

As suggested by Dincer et al. (2021) [30] and IEA (2020) [47], in order to separately account for the effect of costs and revenues related to energy generation, the economic performance of the hybrid energy system is assessed using two different indicators: the *LCOE* and the Levelized Value of Energy (*LVOE*). The *LCOE* [EUR/MWh] provides the production cost of each MWh of electrical power according to the features of the generation system considered. It refers to the expected project lifetime, and it is estimated assuming a constant performance over the lifetime of the system [29].

The *LCOE* is calculated as follows:

$$LCOE = \frac{CAPEX_{WF} + CAPEX_{GTP} + \sum_{t=1}^{T} \left(\frac{OPEX_{WF,t} + OPEX_{GTP,t}}{\left(1+\frac{r}{m}\right)^{m}} \right)}{\sum_{t=1}^{T} \left(\frac{P_{WF,t} + P_{GTP,t}}{\left(1+\frac{r}{m}\right)^{m}} \right)} \tag{11}$$

where T [h] is the total number of hours in the project lifetime. In order to apply Eq. (11), the costs of the hybrid system are needed: $OPEX_{WF,t}$ and $OPEX_{GTP,t}$ [EUR/h] are respectively the operating costs of the WF and of the GTP distributed over the m [h] hours of the reference period. The parameter r [-] is the discount rate referred to the reference period.

The *LVOE* [EUR/MWh] provides the average market price of each MWh produced by a generation system according to the pricing system adopted by the local grid during the sale process. Consequently, the *LVOE* is a metric deriving from the market prices, the incentives and the rules applied by the local TSO to energy delivery. The *LVOE* is calculated as follows:

$$LVOE = \frac{\sum_{t=1}^{m} \left(\frac{R_{BPS,t} + R_{I,t} + R_{unb+,t} - C_{unb-,t} - C_{e_{GHG}}}{\left(1+\frac{r}{m}\right)^{m}} \right)}{\sum_{t=1}^{m} \left(\frac{P_{WF,t} + P_{GTP,t}}{\left(1+\frac{r}{m}\right)^{m}} \right)} \tag{12}$$

where $R_{BPS,t}$ [EUR] is the revenue from the base price power sale, $R_{I,t}$ [EUR] is the contribution of incentives, R_{unb+} [EUR] is the revenue due to the positive unbalances, C_{unb-} [EUR] is the cost paid due to the negative unbalances which are not covered by the GTP, and $C_{e_{GHG}}$ [EUR] is the hourly cost associated to GHG emissions.

It is worth to remark that the economic indicators adopted highlight the cost of energy generation accounting for both capital and operational costs, rather than providing the overall revenue of the investment needed to install the hybrid systems. The latter may be addressed using

conventional methods based on Net Present Value or Internal Return Rate indicators. However, in the framework of the present methodology, the comparison of indicators directly related to the cost of energy generation is considered more effective to assess the economic performance of the alternative hybrid generation systems.

In order to assess the environmental performance of the hybrid system, an indicator considering the Levelized GHG emissions (*LGHG*) [kg_{CO2eq}/MWh] is used [30]. The indicator considers the emissions from the GTP, $e_{GHG,GTP,t}$ [kg_{CO2eq}] over the reference time period, divided by the total energy production:

$$LGHG = \frac{\sum_{t=1}^{m} e_{GHG,GTP,t}}{\sum_{t=1}^{m} (P_{WF,t} + P_{GTP,t})} \tag{13}$$

The above defined indicator has thus a lower value for systems relying mainly on RESs.

The inherent safety indicator adopted to assess the safety performance of the hybrid system is the Levelized inherent Hazard Index (*LHI*) [m^2/MWh], which evaluates the risk of fatalities for the human target due to major accidents per each MWh added by the back-up system. The *LHI* is the sum of the Inherent Hazard Indices HHI_k [m^2/y] associated to each k-th process unit [48] and normalized with respect to the energy produced by the sole GTP:

$$LHI = \sum_{k=1}^{N_{GT}} HHI_k / \sum_{k=1}^{m} P_{GTP,t} \tag{14}$$

HHI_k is referred to each GT, since such items are the only units processing hazardous substances (i.e. NG).

Further details on the calculation of the *LCOE*, *LVOE*, *LGHG* and *LHI* indicators are reported in section A4 of Appendix A.

In order to obtain an easy and clear metric of the overall sustainability performance, suitable for the application in a MCDA framework and useful to produce a ranking of the possible alternatives, a compensatory normalization and aggregation procedure is applied to the above defined indicators [30]. A linear external normalization is adopted, defining two reference values as the upper and lower limits of the range of each indicator (I_{max} and I_{min}). The boundary limits are selected as the extreme values which are unlikely to be exceeded by a wave energy-based offshore hybrid generation system aiming at the valorization of the available RES (the wave resource). In an ideal scenario, such system would not need any back-up power from the GTP. As a consequence, the highest boundary limits correspond to the highest achievable performances of the WF (with respect to the efficiency, the lifetime energy generation, the incentives received and the capability in responding to the dispatching plan without power generation from the back-up system). On the contrary, the lowest boundary limits represent the worst-case scenarios, namely the poor energy conversion performance of the WF or its reduced operation, the low incentives, the high power input from the GTP to compensate the underperformance of the renewable power generation system. The values of the boundary limits are retrieved from the literature, directly or introducing specific assumptions, as shown in Table 2.

Using the values defined for the boundary limits in Table 2, the absolute indicators are re-worked to non-dimensional figures between 0 and 1 with a directionality (0 – undesired, 1 - desired).

Weighing and aggregation are then carried out on the normalized indicators. Weighing is performed using the Analytic Hierarchy Process (AHP) method, which considers the trade-offs among the different metrics according to four different social perspectives [49]. An overall Aggregated Sustainability Index (*ASI*) [-] is thus obtained through Eq. (15) and Eq. (16), where *X* identifies the normalized indicator and *w* the associated weight:

$$ASI = w_{LEE} \bullet X_{LEE} + w_{econ} X_{econ} + w_{LGHG} \bullet X_{LGHG} + w_{LHI} \bullet X_{LHI} \tag{15}$$

where:

Table 3
Data describing the sites selected for the test cases (reference year 2017).

	Adriatic Sea	North Sea
Platform and coordinates	Porto Corsini MW C (44°51′ N, 12°37′ E)	L11b-PA (*L*11-B) (53°28′21″ N, 4°29′23″ E)
Platform's distance from coast and water depth	8 km, 14 m	50 km, 250 m
Platform features (structure type, surface)	4-floors 8-legs, 48 m × 22 m	5-floors 4-legs, 23 m × 20 m
NG rate	4960 Sm^3/h	6685 Sm^3/h
NG composition	CH_4 ~ 100%	CH_4 (93%), ethane (3%), CO_2 (2%) and N_2 (2%)
Buoy and coordinates	Nausicaa (44°21′ N, 12°48′ E)	L91 buoy (53°61′ N, 4°96′ E)
Buoy's distance from coast and water depth	8 km, 10 m	50 km, 250 m
Wave data source	[56]	[57]
Data series type	30-minutes series	10-minutes series
Available data %	72	96
References	[58,59]	[60,61,62]

$$X_{econ} = w_{LCOE} \bullet X_{LCOE} + w_{LVOE} \bullet X_{LVOE} \tag{16}$$

The approach used for the normalization and to derive the weighing coefficients is reported in section A5 of Appendix A.

Finally, when the comparison of alternative sites or of alternative setups is of interest, a sensitivity analysis is applied to the ranking of alternatives based on the figures obtained for the aggregated sustainability indicator. Indeed, uncertainties might affect the procedure, mostly due to the variability of input data, to the normalization applied, to the weighing parameters selected. Therefore, carrying out a sensitivity analysis is advisable in order to identify possible aberrations and to verify the robustness of the final ranking. The Monte Carlo method is here proposed for application as it enables the random variations of multiple key variables in a high number of iterations [53].

The outcome of the methodology is thus the conceptual design of a sustainable hybrid generation system optimized for the exploitation of RESs in the site of interest, based on a design value of the probability of correct dispatching and on sustainability KPIs used for performance assessment of alternative design options.

More in detail, the application of the methodology provides the identification of the most suitable WEC to be deployed, as well as the number of these devices that need to be installed according to the nominal potentiality of the wave farm and to design constraints. Based on the simulation of the real and of the forecast performance of the renewable system, the dispatching plan is obtained. Thus, the method also enables the conceptual design of the back-up GTP, in terms of type and number of machines and the definition of the GTP operating plan on the basis of the dispatched power curve. The set of KPIs provided allows the quantitative assessment of the broad sustainability of the hybrid system defined.

3. Case studies

Two sites were selected to carry out case-studies aimed at demonstrating the applicability and the results obtained from the developed methodology. The selected locations are characterized by intense offshore extraction activities, the North Sea being the cradle of several oil&gas fields, while the Northern Adriatic Sea hosts plenty of NG reserves. Furthermore, Italy is the country which mostly employs WECs prototypes in the Mediterranean area, with the Northern Adriatic being the test basins of several offshore devices [54], while North Sea is an attractive region for WEC installation due to the high wave potentials (5 to 10 kW/m [55]).

A preliminary assessment of the wave energy potential in the test sites evidenced important differences, along with the site characteristics [55].

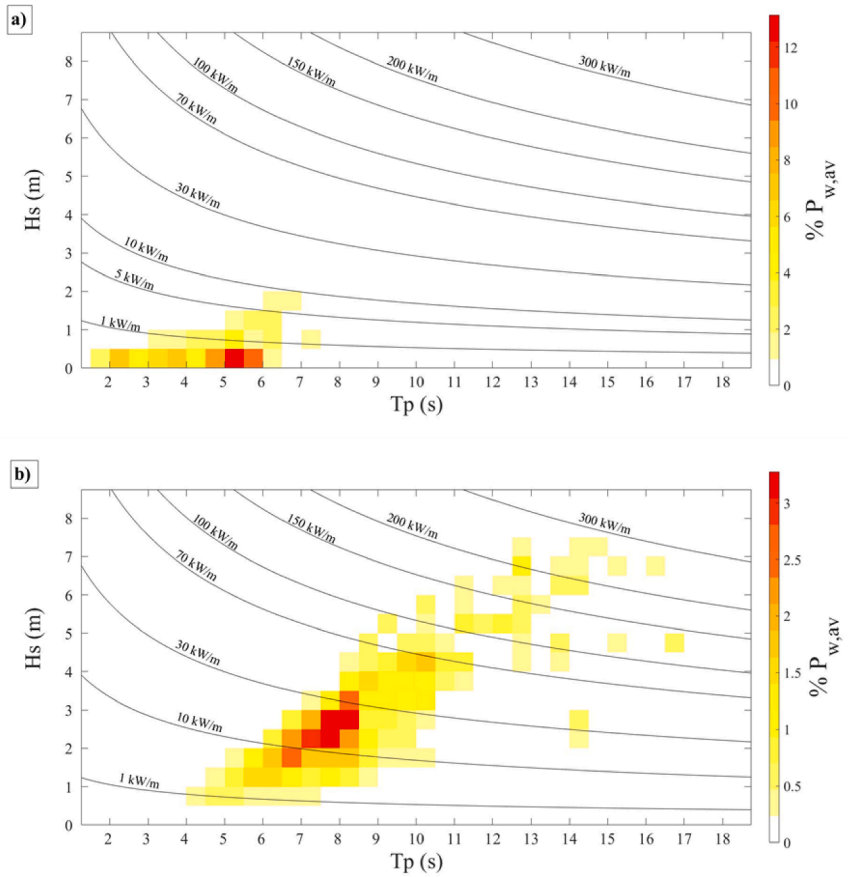

Fig. 2. Bivariate distributions of yearly occurrences of (T_p, H_s) in 2017 in: (a) the Adriatic Sea test site; (b) the North Sea test site. The color scale represents the contribution of each bin to the total incident energy, as a percentage. The wave *iso*-power curves are also reported.

In both locations an existing extraction rig is considered for the possible installation of the G2P system providing a back-up to a 2 MW nominal capacity WF. The probability of correct dispatching is set equal to 80% for the reference case assessment (scenario A), thus fulfilling the requirements of step 0 of the proposed methodology (see Fig. 1).

The data collection (step 1 of the methodology) is then performed.

Table 4
Performance parameters obtained for the five WECs selected in the test-cases based on the available reference year meteo-marine data. The referenced sources report the technical specification of the WEC devices considered in the present study.

	Pelamis	Aqua BuOY	Lysekil WEC with 2 m-stroke	Lysekil WEC with 4 m-stroke	Wave Dragon prototype 1:1.5
Reference	[50]	[50]	[65]	[65]	[50;66]
Adriatic Sea					
AEP_{WEC}[MWh]	11.4	5.4	1.4	1.4	83.0
$\overline{P}_{WEC}$[kW]	4.7	2.2	0.6	0.6	34.1
CF	0.01	0.01	0.02	0.01	0.04
CW[m]	4.7	2.2	0.6	0.6	33.9
Overall performance ranking	0.09	0.06	0.13	0.06	1.00
North Sea					
AEP_{WEC}[MWh]	794.5	199.6	28.9	32.0	1959.4
$\overline{P}_{WEC}$[kW]	90.7	22.8	3.3	3.6	223.7
CF	0.12	0.09	0.12	0.08	0.23
CW[m]	11.6	2.9	0.4	0.5	28.6
Overall performance ranking	0.36	0.08	0.07	0.00	1.00

Table 3 summarizes the main data concerning the two sites for the reference year selected (2017). In the case-studies carried out, the reference year was selected on the basis of the availability of the required input data.

Fig. 2 reports the energy contribution of each bin to the total yearly wave energy according to actual data obtained for the two sites. The average wave potentials calculated are of 1 kW/m and 7.8 kW/m for the Adriatic and North Sea cases, respectively. These values are coherent with the findings of Mørk et al. 2010 [55] (<5 kW/m for the Adriatic Sea and 5–20 kW/m for the North Sea). Further information about the sites considered is reported in Appendix B.

WECs data is retrieved for the devices that could be installed in both sites, i.e., Pelamis, Aqua BuOY, Lysekil WEC (either with 2 m or 4 m strokes) and the down-scaled device 1:1.5 of the Wave Dragon (WD).

Some assumptions were introduced in the assessment of the case-studies:

- the nominal capacity of the hybrid energy plants is selected equal for the two sites in order to allow a significant comparison;
- the same GT model, plant size and forecast horizon are selected in the two sites in order to reduce the number of diverging input parameters and to capture the influence of the exploited RESs;
- the rig, the well and the measurement buoy are considered close to each other. The actual distances between the buoy and the WF installation are supposed to have a negligible influence on the variables related to wave motion across the same geographical area;
- the lifetime considered for the two hybrid energy generation systems is 20 years;
- for the sake of simplicity, the technological and economic performances in the reference year are assumed constant for the entire

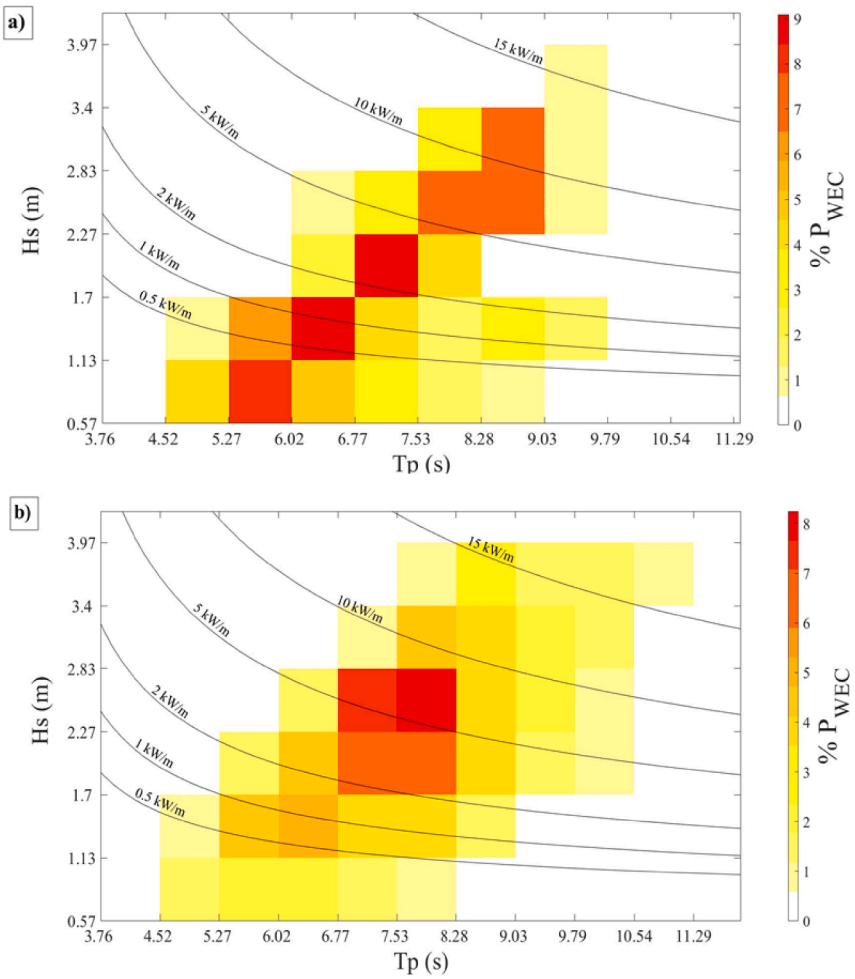

Fig. 3. Scatter diagrams reporting the power production frequencies obtained for the application of the selected Wave Dragon device in the test sites: a) Adriatic Sea; b) North Sea.

lifetime. Nevertheless, for more accurate evaluations, the application of a regional assessment considering the future conditions of the natural resources, as the one presented by Lira-Loarca et al. (2021) [63], is suggested.

In order to understand if any important modification of the results with respect to the reference scenario A (80% probability of correct dispatching) occurs when model parameters are changed, two further scenarios are introduced:

i) the declared dispatching accuracy is improved to 90% (scenario B);
ii) lower WEC costs are assumed due to full scale commercialization, as suggested by Sørensen and Friis-Madsen (2014) [64] (scenario C).

4. Results and discussion

4.1. Conceptual design of the hybrid generation system for the test cases

Table 4 shows the values of the performance indicators obtained from the simulation of the alternative WEC technologies considered in the two test sites, as per step 2a of the methodology. The studies referenced in Table 4 report the technical specifications and the power matrices of each WEC, that were used in the performance evaluation.

Table 4 also reports the performance indicators calculated for the different WECs by the procedure described in section 2.2.1. As shown in the table, the WD converter was found to be the best-performing WEC technology in both sites.

Table 5
Summary of the results of the conceptual design of the hybrid generation system in the two test sites.

	Adriatic Sea	**North Sea**
Selected WEC	Wave Dragon prototype 1:1.5, $P_{WEC,nom}$ = 0.96 MW	Wave Dragon prototype 1:1.5, $P_{WEC,nom}$ = 0.96 MW
P_{WF} [MW]	1.9	1.9
N_{WECs}	2	2
Selected GT	Microturbine Capston, $P_{GT,nom}$ = 200 kW	Microturbine Capston, $P_{GT,nom}$ = 200 kW
P_{GTP} [MW]	2	2
N_{GT}	10	10

Nevertheless, as expected, the difference in the power output is relevant between the two sites: the AEP_{WEC} associated to the North Sea is 6.5 times higher than the one obtained in the Adriatic Sea. The power production frequencies of the 1:1.5 WD prototype are reported in Fig. 3 in terms of operative bins (H_s, T_p) for both sites. The figures allow the identification of the most frequent operating conditions. Notably, in the Adriatic Sea, the WD produces energy in a narrower range of T_p conditions and presents some powerful operative bins. On the contrary, in the North Sea, the same device operates in multiple sea conditions, but its higher power contribution occurs with more powerful sea states (H_s and T_p ranges are 1.5–2.5 and 6.5–8, respectively).

On the basis of the design capacity assumed for the WFs (2 MW), in each test site the hybrid energy system consists of 2 WECs (P_{WF} = 1.92

Table 6
Technological, economic, environmental and inherent safety performances of the hybrid generation plants for the two case-studies considering scenario A.

TECHNOLOGICAL PERFORMANCE				
			Adriatic Sea	**North Sea**
Wave Farm	Available wave energy yearly	*MWh*	1143	8875
	Nominal Power	*MW*	1.92	1.92
	Electrical energy produced yearly	*MWh*	598	3919
	EFLH	*h*	312	2044
	h_{WF}	*h*	1648	6450
	Percentage h_{WF}	–	19%	74%
	Average η in h_{WF}	–	70%	68%
GTs park	Nominal Power	*MW*	2.00	2.00
	Electrical energy produced yearly	*MWh*	54	415
	EFLH	*h*	27	207
	h_{GT}	*h*	198	830
	Percentage h_{GT}	–	2%	9%
	Average η in h_{GT}	–	31%	31%
Hybrid System	Nominal Power	*MW*	3.92	3.92
	Electrical energy produced yearly	*MWh*	651.6	4333.6
	Thermal Energy input	*MWh*	172	1300
	LEE	–	14%	53%
ECONOMIC PERFORMANCE				
			Adriatic Sea	**North Sea**
Revenues from renewable energy incentives R_I		*EUR*	134,135	344,848
Revenues from sales at base market price R_{BPS}		*EUR*	46,085	171,301
Total from sale A = $R_I + R_{BPS}$		*EUR*	180,220	516,149
Revenues / Costs from unbalances	R_{unb+}	*EUR*	9600	0
	C^-_{unb}	*EUR*	−850	0
	$B = R_{unb+} + C^-_{unb}$	*EUR*	8750	0
Emissions penalties	C_{GHG}	*EUR*	0	0
Total = A + B-C		*EUR*	188,970	516,149
LVOE		*EUR/MWh*	290	119
LCOE		*EUR/MWh*	3960	610
ENVIRONMENTAL PERFORMANCE				
			Adriatic Sea	**North Sea**
Total emissions		ton_{CO2eq}	31.9	240.5
LGHG		kg_{CO2eq}/MWh	48.9	55.5
INHERENT SAFETY PERFORMANCE				
			Adriatic Sea	**North Sea**
HHI		m^2/y	6.15E-03	3.75E-02
LHI		m^2/MWh	1.14E-04	9.03E-05

MW). The P_r and P_f curves are obtained as discussed in step 2a of the methodology. Consequently, step 2b can be applied for the quantification of the dispatching errors $\xi(t)$, in order to derive the P_d curves in each site. Based on the dispatch schedules defined, the potentialities needed from the back-up systems are found. The results show that both in the Adriatic and North Sea, 2-MW GTPs are needed. A total of 10 aero-derivative machines rated 200 kW each were selected for each GTP [23], as summarized in Table 5.

4.2. Sustainability assessment of the test-cases

Once consolidated the design of the hybrid system, step 3 of the methodology is applied. Table 6 shows the values of the sustainability indicators calculated for the two test cases analyzed. As far as the technological performance is concerned, the limited operating time and the low energy production in the Adriatic Sea test site result in only 312 Equivalent Full Load Hours (EFLH), with respect to the 2044 EFLH calculated for the North Sea test case. Therefore, although the intensive performance of the device in the Adriatic site during its few working hours (demonstrating an average η of 70%), the difference in the *LEE* values is clear (53% vs 14%), being the operation of the WDs more extended in the North Sea than in the Adriatic Sea. Even if the results are difficult to benchmark due to the specific power levels, the values obtained are similar to those reported by the comprehensive study carried out by Pecher (2013) [67].

With respect to economics, the cost items for the down-scaled WDs are retrieved from the specialized literature [68]. CAPEX and OPEX of the 200-kW GTs amount to 3150 EUR/kW and 20 EUR/MWh, respectively [69]. All cost items were updated to the reference year (2017) using the Consumer Price Index for the European zone. It should be remarked that no emission costs are charged, as the two plants are classified as "small emitters" (i.e. < 25 kton of CO_2 per year) according to the European Emission Trading System [70]. The low energy generation in the Adriatic Sea test site is responsible for a *LCOE* value as high as 3960 EUR/MWh, about six times higher than the value obtained for the North Sea test site (610 EUR/MWh). The *LCOE* figures obtained for the North Sea test site are aligned with the findings of de Andres et al. (2016), who reported values from 500 to 1600 EUR/MWh for large wave farms in the North Sea [71], as well as with the values reported by Foteinis and Tsoutsos (2017) [13] for small wave farms.

Clearly enough, wave energy-based hybrid systems still have a too high *LCOE* to be considered competitive with respect to other generation sources, especially in the case of the Adriatic Sea. However, the *LVOE* results are promising, highlighting the presence of favorable pricing rules concerning wave energy-based power systems connected to the local grids considered in the test cases. The *LVOE* is higher of a factor of about 2.5 in the Adriatic Sea test case, as a consequence of the higher incentives applied in Italy.

It is interesting to compare the performance of the hybrid system to that of the sole wave farm considering three main parameters: the *LCOE*, the *LVOE* and the dispatchability of energy. The complete results concerning the performance of the WF in the absence of the GTP are reported in Appendix C. As expected, the exclusion of the back-up GTP implies a slightly improved economic performance in the test cases considered. Indeed, the *LCOE* decreases to 3600 EUR/MWh and 563 EUR/MWh respectively in the Adriatic and North Sea. The reduction in the *LCOE* highlights that the GTP installation requires an additional cost in front of a reduced contribution to the energy generation, since the GTP operation strategy aims at the increase of the energy dispatchability, not at the increase of energy generation. This is clearly shown in Fig. 4 that reports the power trends of both the WF and the GTP in the North Sea test case on a sample time period.

Differently, the LVOE increases to 306 and 128 EUR/MWH in the Adriatic and North Sea, respectively, when only the WF installation is considered. The increase in the *LVOE* obtained for a fully-renewable system is due to the power pricing patterns, that are not only dependent on the amount of energy generated, but are rather influenced by both the adjustment of generated power to the declared dispatching curve and the pricing that the TSO assigns hourly to the energy dispatched to the grid.

Finally, it should be remarked that the reduced *LCOE* and the null values of *LGHG* and *LHI* associated with the WF in the absence of the GTP come in front of a reduced dispatchability of the energy generated. Actually, the WF alone fails to comply with $Prob_d$, the probability of correct dispatching, which was set to assure a stable power supply in the

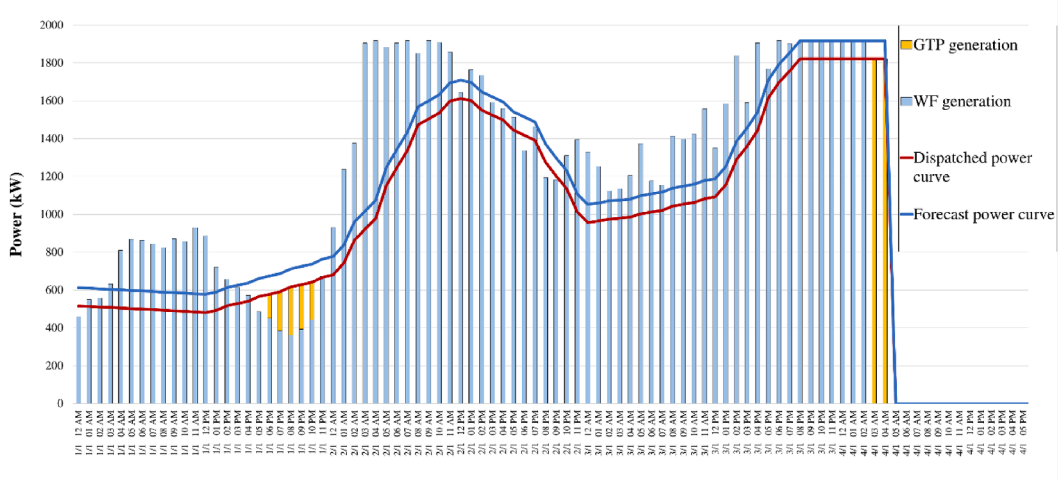

Fig. 4. Forecast and dispatching power curves obtained for the North Sea hybrid system (scenario A) along with the power generation trends from the WF and the GTP for a sample period of the reference year.

grid. In the Adriatic Sea case, the reduction of 9% in the *LCOE* obtained excluding the GTP occurs with a slight decrease of the probability of correct dispatching (from 78% to 77%). In the North Sea test case, the *LCOE* drops by 8%, but the probability of correct dispatching decreases from 77% to 71%.

Concerning the environmental impacts, the equivalent GHG emissions depend on the GTP dynamic operation, which in turn depends on the need of compensation between the dispatched and real power curves hour by hour. The *LGHG* is similar for the two sites, with the Adriatic Sea test case performing better than the North Sea one because of the slightly more accurate forecast. The figures obtained are lower than the values expected for micro-gas turbines [72], due to the definition of *LGHG*, which distributes the equivalent CO_2 emitted on both the renewable and fossil-based generations.

Similarly, the inherent safety of the two hybrid plants is influenced only by the operation time of the GTs, since the features and sizes of the two GTPs are equal for the two test cases. The Adriatic Sea test site, due to the fewer operation hours of the GTP, features a lower inherent risk (see the absolute inherent risk indicator *HHI* in Table 6). However, the *LHI* ranking is reversed because of the higher energy generation occurred in the North Sea test case, as per Eq. (14). More in general, the *LHI* values are aligned with those obtained in similar studies targeting the conversion of offshore platforms [46].

The improvement of the probability of correct dispatching from 80% to 90% (scenario B in section 3) causes the increase of ξ_d in every month of the year. However, this phenomenon has different effects in the two test cases analyzed, as shown in Fig. 5-(b). In the North Sea test site, almost negligible variations affect the cost items due to the presence of relevant forecast errors. In the Adriatic Sea test case, the enhanced forecasting causes the dispatching plan to diverge to a larger extent from the generation curve due to real-weather conditions, with two opposite effects: higher revenues caused by the positive unbalances but also higher costs due to the negative unbalances.

With respect to the possible future reduction of WEC costs (scenario C in section 3), Fig. 5-(c) shows that, as expected, a relevant reduction of CAPEX and OPEX (68% and 73% respectively) will have a favorable impact on the process economics: the *LCOE* drops to 1300 EUR/MWh and 248 EUR/MWh for the Adriatic Sea and North Sea sites respectively, with a higher relative benefit for the first site. The different impact of the reduced OPEX in the two sites is due to the different operation of the wave farms in the two locations.

The normalized indicators calculated for the two test cases considering scenario A are displayed in the radar plot of Fig. 6. Apart from X_{LGHG} and X_{LHI}, which are aligned, X_{LEE}, X_{LVOE} and X_{LCOE} score very different values in the two case studies. It should be remarked that X_{LCOE} is zero for the application in the Adriatic Sea since its non-normalized value exceeds the maximum considered for the normalization range, that is, it exceeds the maximum *LCOE* expected for WECs nowadays. This result is consistent since the *LCOE* is calculated on the basis of the costs of energy generation, thus it is strongly dependent on the performance of the renewable energy system in each location. Differently, the upper limit considered for the normalization is the maximum figure available in the literature for commercially deployed wave energy projects, thus it concerns projects where the economic viability was confirmed.

Overall, the North Sea test case demonstrates a higher performance than the Adriatic Sea test case, as confirmed also by the values of the four ASI indicators, reported in Fig. 7-(a), which were calculated according to the four weighing approaches considered.

The ranking of the alternatives is unchanged when applying different social perspectives (i.e. different weighing modes) to the calculation of the overall sustainability indicator, ASI. Fig. 7-(b) reports the ASI metrics obtained for scenario B, i.e. when the improvement of the correct dispatching to 90% is applied, together with their percentage variations with respect to the baseline scenario. The ranking of the test sites is unchanged. In the case of the Adriatic Sea, the ASI always increases for any social perspective considered. In the North Sea test case, the aggregated results are worsened when considering the Individualist and Equal Weight ASI. The lower ASI values obtained by these weighing approaches are mainly due to both the decrease of the *LEE* and the increase of the *LCOE*. The former is caused by the prolonged intervention of the GTP, thus by the higher influence of the GT efficiency on the *LEE*. The latter is related to the reduced energy delivery, as a consequence of a more measured back-up system generation due to the optimized forecast and dispatching.

The North Sea test case provides the best performance, even in scenario C (reduction in the commercial prices of the WF), as shown in Fig. 7-(c). In both sites, only positive variations of ASI are recorded. Also in this case, the Adriatic Sea test case shows a higher relative improvement. The Individualist and the Equal Weight weighing approaches are influenced by cost reductions to a larger extent than the other weighing modes, since these approaches give a notable consideration to the stakeholder's economic convenience.

Fig. 8 shows the outcome of the sensitivity analysis, aimed at verifying the robustness of the sustainability ranking based on the ASI indicator.

In detail, the Monte Carlo method was applied to some critical input parameters for 10^6 iterations, assuming their variation according to both

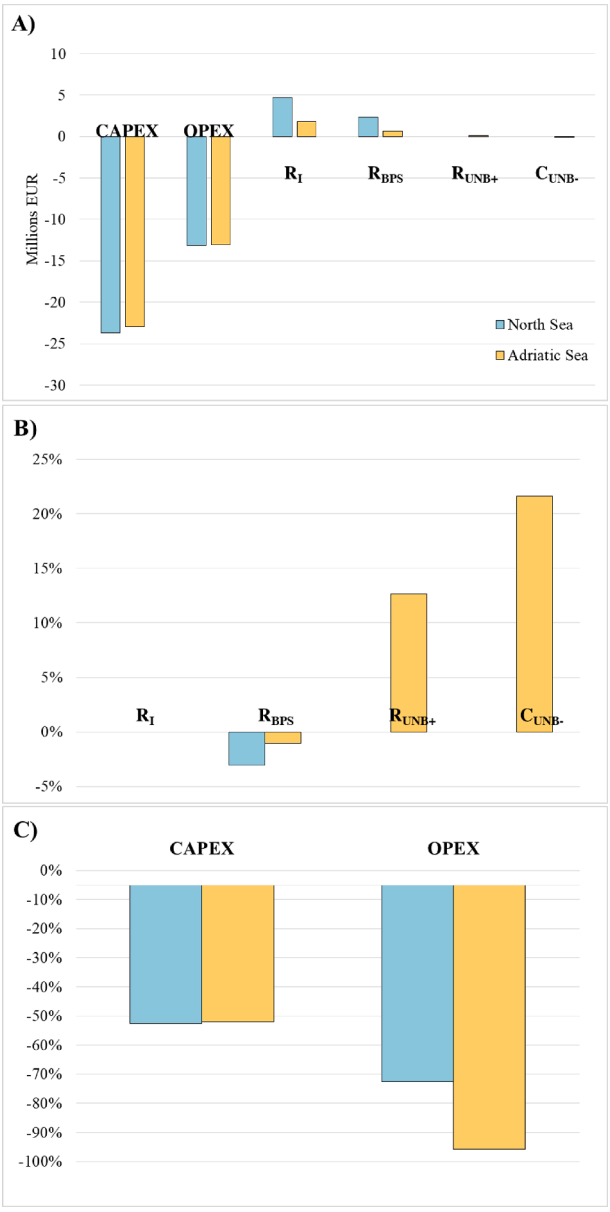

Fig. 5. Costs and revenues for the Adriatic Sea and North Sea test cases: a) scenario A; b) differences calculated when considering scenario B with respect to scenario A; c) differences calculated when considering scenario C with respect to scenario A (see Section 3).R_I = total revenues from incentives, R_{BPS}= revenues from base price sale, R_{unb+}= revenues due to positive unbalances, C_{unb-}= costs due to negative unbalances.

the uniform and the beta distribution ($\alpha = \beta = 2$) in defined existence ranges. The most critical parameters are those which are subject to the analyst decision and perception. Therefore, the two extremes of the normalization range as well as the aggregation weights for each sustainability metric are variated: the former in a range +/- 50% of the original values, the latter with the constraint to sum up to 1. The CDF curve of the beta distribution was calculated for the differences between the North Sea (ASI_N) and the Adriatic Sea (ASI_A) aggregated indicators. In the baseline case (scenario A in section 3), this difference is positive.

The obtained CDF curves confirm that a robust ranking was provided and that its inversion has a negligible probability of occurrence. Notably, the robustness of the results is also confirmed when considering, more conservatively, a uniform distribution for the variation of the target parameters (red curve in Fig. 8).

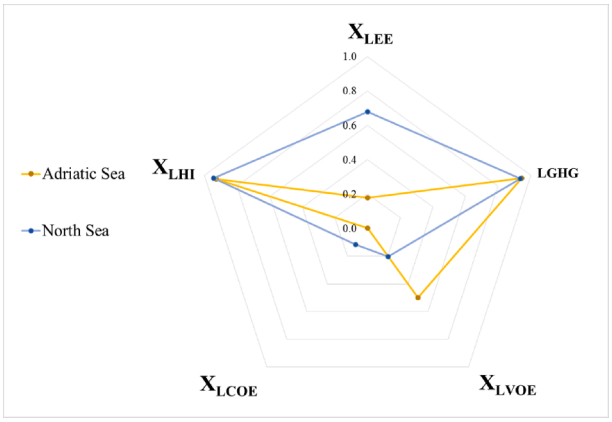

Fig. 6. Normalized sustainability indicators calculated for the two test sites considered in scenario A.

4.3. Discussion

The proposed methodology uses the forecast-based dispatching curve and a user-defined probability of correct dispatching to support the conceptual design of offshore hybrid power generation systems exploiting wave energy in combination with a natural gas fueled back-up system aimed at valley filling. The proposed design procedure allows the system to comply with the WF capacity and with the probability of correct dispatching, thus fulfilling the main TSO requirements for the supply of renewable energy in the grid. The wave resource exploitation is designed by a specific step addressing the selection of the WEC technology, following the simulation of the device performance over real site-specific meteo-climatic data. Basing the back-up generation system design on the probability of correct dispatching avoids oversizing of the system and allows a flexible operation of the GTP. The final sustainability assessment, which resulted robust as per the sensitivity analysis, provides an *a posteriori* evaluation of the conceptual design proposed, that allows the performance comparison of alternative options suitable for wave energy harvesting which have been previously identified as viable based on a preliminary scouting.

Thus, the sustainability footprint and overall index obtained from the method address the identification of the most sustainable configuration of an offshore wave-based generation plant with respect to the wave potential and to the best operational adaptability to the grid requirements.

Within the sustainability assessment, costs represent an important issue. In the analysis of the test cases, no difference was introduced in the single cost items considered for the two test cases. Actually, even if two different geographical areas are compared (Adriatic and North Sea), it should be noted that they belong to the same economic area. In addition, the capital costs related to offshore projects undergo the dynamics of the global market, while operative costs, which are more influenced by regional factors, have a lower influence on the results. However, in perspective, if sites in geographical areas having different levels of economic development are compared, the methodology should be extended to include cost correction factors taking into account the different offshore operational theaters considered for the installation of the hybrid system.

Nevertheless, the cost figures obtained in the test cases show that a hybrid generation system obtained coupling a renewable generation system to a GTP, operated with a strategy aiming at increasing the stability of the energy supplied to the grid and to minimize the energy generation from the GTP, results in a *LCOE* higher than that of the renewable system alone. However, when calculating the *LCOE* of renewable energy generation systems, the overall costs of grid balancing are usually not considered. Further work will thus be needed to fully understand the actual economic performance of hybrid systems when

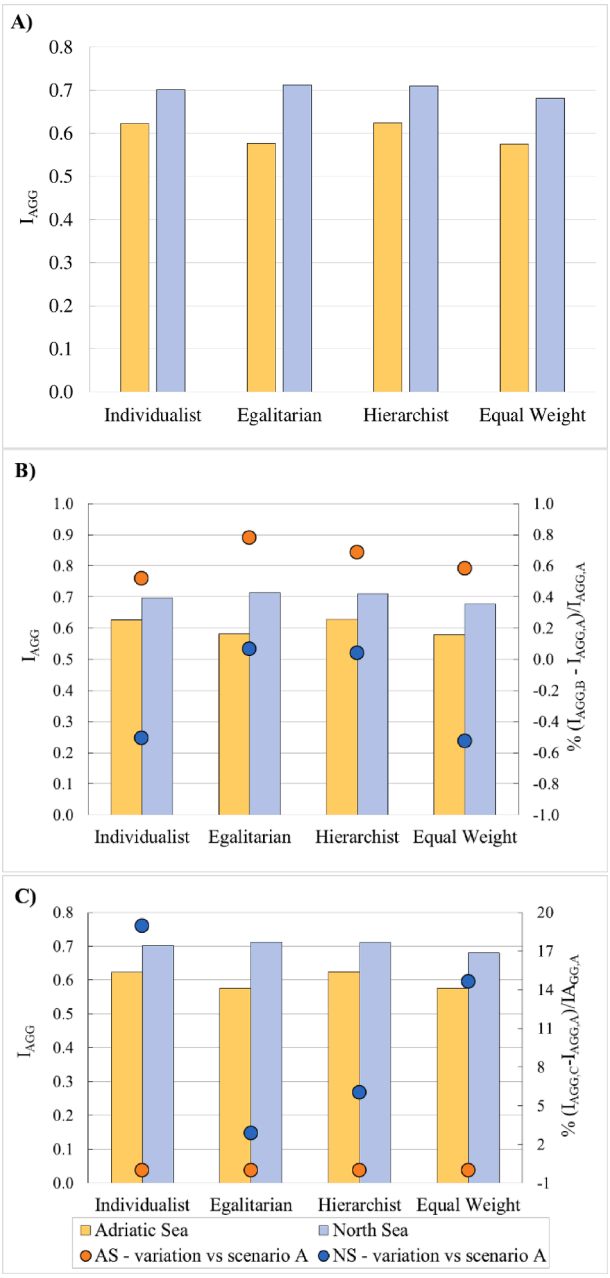

Fig. 7. ASI results according to the four decision-making perspectives: a) scenario A; b) scenario B; c) scenario C.

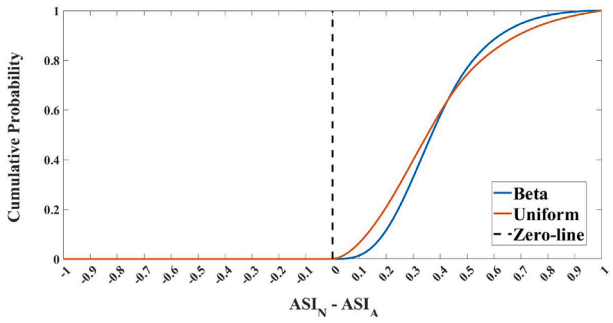

Fig. 8. CDF of the difference between the ASI index calculated for the North Sea test case (ASI_N) and that calculated for the Adriatic Sea (ASI_A) resulting from the sensitivity analysis where error probabilities were simulated using a uniform (red curve) or a beta ($\alpha = \beta = 2$, blue curve) distribution.

taking into account the costs related to the grid balancing and to the stabilization of energy supply.

5. Conclusions

A systematic methodology to support the conceptual design of wave energy hybrid systems and to assess their sustainability performance from the technological, economic, environmental and process safety viewpoints is proposed. The method is demonstrated by its application to two test cases, where hybrid solutions are tested for wave energy valorization in the Adriatic Sea and in the North Sea. The hybrid generation systems defined applying the developed methodology perform differently in the two sites, due to differences in the available wave energy resource and in the forecasting accuracy. The annual energy production resulted 6.5 times higher in the North Sea test-case. Conversely, the low energy generation in the Adriatic Sea test site results in a levelized cost of energy of 3960 EUR/MWh, much higher than the value of 610 EUR/MWh obtained for the North Sea. In both cases, the installation of the gas turbine park impacts negatively on the cost of energy production but is of crucial importance in meeting the design value of the probability of correct dispatching.

The application of the multi-criteria method developed allows the quantification of the system response under each sustainability aspect, highlighting site-specific strengths and weaknesses. The sustainability ranking obtained highlights the best performance of the North Sea test site. The robustness of the sustainability ranking was confirmed by a multi-variable Monte Carlo analysis. The developed methodology is intended as a support for the development and design of hybrid generation systems based on the exploitation of wave energy. Its novelty is in the inclusion of an appropriate interface modulation between renewable generation and the grid owners, aimed at avoiding technical issues and at maximizing the dispatching accuracy by the definition of a target probability for correct dispatching. The assessment of the dispatching plan and the back-up system management strategy approached by the methodology also allow unveiling economic aspects related to the operation of the system, thus providing a comprehensive support to the decision-making process in the conceptual design stage of the project lifecycle.

CRediT authorship contribution statement

Mariasole Cipolletta: Conceptualization, Investigation, Methodology, Writing – original draft. **Anna Crivellari:** Conceptualization, Investigation, Methodology. **Valeria Casson Moreno:** Conceptualization, Methodology, Validation, Writing – review & editing. **Valerio Cozzani:** Conceptualization, Writing – review & editing, Supervision.

Declaration of Competing Interest

The authors declare that they have no known competing financial interests or personal relationships that could have appeared to influence the work reported in this paper.

Data availability

Data will be made available on request.

Appendix A:. Specific details of the methodology

Real vs forecast data

Real data are in-situ measurements derived from specific devices located at the offshore site or in the close vicinity. Based on the type of instrument and recording technique used, wave climate parameters can

Table A1
Main scaling rules based on scaling factor λ for WECs at different sites [38].

Parameter	Relation	WEC ($\lambda = L_1/L_2$) Scale dependence
WEC power production P_{WEC}	$P_{WEC,1}/P_{WEC,2}$	$\lambda^{7/2}$
Significant wave height H_s	$H_{s,1}/H_{s,2}$	λ
Wave period T_m or T_p	$T_{m,1}/T_{m,2}$ or $T_{p,1}/T_{p,2}$	$\lambda^{1/2}$

be obtained as average values of the wave parameters for short-term statistics (from seconds to hours according to the measurement principle of the device) [67]. Bivariate distributions of occurrences corresponding to different combinations of H_s and T_m (or H_s and T_p) – hereafter called bins - can be also derived and visualized as scatter diagrams. A less cumbersome way to describe wave conditions is to group bins into a limited number of zones, referred to as "sea states", on the basis of H_s and T_p values of interest in a specific marine location [67]. Concerning wave forecasting, two major methods can be distinguished: physics-based and time series models [73]. The comparison between physics and time series models showed statistical methods are more accurate than physic models over limited time spans (1–4 h) [21], while for longer forecasts physics-based methods tend to produce more reliable results, provided that the convergence point between the two techniques for comparable accurate results is around 6 h forecast horizon [35].

Time horizons between 3 and 6 h enable to meet the variations in production and to control the capacity at the system operators' disposal.

Furthermore, for an improved dispatching, the time horizon for forecasting should be consistent with the market operation constraints [74] that vary worldwide, e.g. (about 6 h in the United States of America, Canada and UK [75], 4–5 h forecasts in Europe while 2–3 days ahead are used to determine the available reserves for the day-ahead market [73]).

Theory and scaling of WECs

The knowledge of the performance of the WECs is essential.

Typically, a performance matrix is provided by the constructors reporting the produced power as a function of bins (H_s, T_m) or (H_s, T_p) [58]. Power matrices may refer to the net electrical power output of the WEC (P_{WEC}) or to the power absorbed by the device ($P_{w,abs}$); in the latter case, power-take-off and generator efficiencies (η_{PTO} and η_{gen}) should be considered to account for the conversion of absorbed power into rotating mechanical power and for the transformation of rotating mechanical power into electrical power [76]. Power matrices are derived from experimental data or numerical simulations for given operating conditions based on the working principle of the device [67].

During the primary conversion of marine energy inside the WECs, gravity and inertial forces are dominant and the effect of remaining forces (such as kinematic viscosity) are negligible, thus mechanical similarity is achieved by the Froude's scaling law between model and prototype devices [77]. The scaling factor λ, based on Froude similitude, is the ratio between the characteristic lengths L_1 of the reference device and L_2 of the scaled device: by varying the capture width, the output power changes, but the device's response keeps constant with the spread over the frequency range [38]. Table A.1 shows the scale dependence of all parameters of a down-scaled power matrix [39].

GTs part-load efficiency

Depending on the GT category, the efficiency reduction at part-load can be expressed as a function of the part-load ratio (power produced at part-load, P_{GT}, against $P_{GT,nom}$).

For aero-derivative GTs, the following correlation proposed in the literature [43] is used in the present methodology:

$$\frac{\eta_{GT}}{\eta_{GT,nom}} = 0.7035 \bullet \left(\frac{P_{GT}}{P_{GT,nom}}\right)^3 - 1.91151 \bullet \left(\frac{P_{GT}}{P_{GT,nom}}\right)^2 + 2.0642 \bullet \left(\frac{P_{GT}}{P_{GT,nom}}\right) + 0.1481 \quad \text{(A1)}$$

For micro GTs, a proper correlation is derived in the present work by regressing the part-load efficiency curve of commercial micro GTs by Capstone Turbine Corporation (C800 and C330 models) [78,79], expressed as follows:

$$\frac{\eta_{GT}}{\eta_{GT,nom}} = 2.1812 \bullet \left(\frac{P_{GT}}{P_{GT,nom}}\right)^3 - 4.6655 \bullet \left(\frac{P_{GT}}{P_{GT,nom}}\right)^2 + 3.4475 \bullet \left(\frac{P_{GT}}{P_{GT,nom}}\right) + 0.0584 \quad \text{(A2)}$$

Among the possible control strategies proposed in the literature for GTs [80–84], the approach suggested by Guandalini et al. [43] is adopted in the present study, which consists in managing each GT of the park in parallel at the same part-load. Starting from the full-load condition of the park, if the load decreases all machines reduce equally their load up to the condition at which one machine can be switched-off and all remaining machines return to operate with their $P_{GT,nom}$. The strategy proceeds equally in the case of other load decreases, until one sole machine remains in operation before reaching its minimum technical load, which is set at 50% of $P_{GT,nom}$ in order to meet the environmental limits on CO and NO_x commonly imposed in the technical specifications.

Details for the calculation of sustainability indicators

A4.1 LCOE

The LCOE is calculated starting from preliminary estimates of capital expenditures (CAPEX), operating expenditures (OPEX) of the hybrid plant, thus of the wave farm and the associated back-up system. CAPEX and OPEX associated to the GT plant for aero-derivative and micro GTs are available in the literature [85,86,87].

A4.2 LVOE

Dealing with electricity sale, the market prices for renewable power can vary depending on the pull mechanism adopted at national level for the promotion of RESs participation into the grid (e.g. feed-in tariff, feed-in-premiums, quota-based tradable green certificates, investment subsidies or tax cuts) that are added to the electricity base price. Clearly enough, eligibility requirements to receive support should be verified according to the current national regulations.

Therefore, market base prices of electricity ($Price_{el,base}$) are retrieved with particular attention to possible incentives launched at national level for the promotion of RESs and related eligibility requirements. Furthermore, based on the local regulations to control power unbalances, producers may receive incentives ($Price_{unb+}$) when power injection is higher than the declared one, but, on the contrary, may also pay fines ($Price_{unb-}$) in case of negative unbalances [43]. Thus, prices established by the local TSO for positive and negative power unbalances need to be collected.

Finally, the price associated to GHG emissions from the GTP is retrieved: it may be a carbon allowance total direct GHG emissions from specific sectors in a cap-and-trade system (e.g. emission trading scheme or ETS) or a pre-defined carbon tax on GHG emissions based on the policy adopted by local governments [88]. Information about the regional, national and subnational carbon pricing initiatives implemented, scheduled and under considerations, including the associated prices, is published every year by the World Bank [89]. The revenue and cost items composing LVOE are detailed in the following equations.

$$R_{sale,t} = Price_{el,base} \bullet P_{GT,t} + Price_{el,RES} \bullet P_{WF,t} = R_{BPS,t} + R_{I,t} \tag{A3}$$

$R_{sale,t}$(in Eq. A3) is the total revenue from electric sale through grid feed-in. Within total revenues from sale, a distinction can also be made between revenues from base price power sale $R_{BPS,t}$ and the ones only due to incentives $R_{I,t}$. $Price_{el,base}$ is the market price [EUR/MWh] of conventionally generated energy and $Price_{el,RES}$ [EUR/MWh] is the market price of each MWh of renewable energy supplied to the grid, comprehensive of possible incentives.

Eq. A4 and Eq. A5 show the calculations for the hourly revenues and costs from positive and negative unbalances, respectively:

$$R_{unb+,t} = Price_{unb+} \bullet P_{unb+,t} \tag{A4}$$

$$C_{unb-,t} = Price_{unb-} \bullet P_{unb-,t} \tag{A5}$$

where P_{unb+} and P_{unb-} are the average powers unbalanced in the t-th hour, respectively in excess and in defect with respect to P_d according to the dispatching plan.

GHG emission costs $C_{GHG,t}$ at t-th hour depend on the monetary fines imposed over CO_2eq emissions ($Price_{GHG}$ [EUR/$kg_{CO2,eq}$]) and the hourly emissions from the GT park $e_{GHG,GT}$ [kg_{CO2eq}] as per Eq. A6:

$$C_{GHG,t} = Price_{GHG,t} \bullet e_{GHG,GT,t} \tag{A6}$$

A4.3 LGHG

GHG emissions for the hybrid plant are estimated for the calculation of LGHG, provided that the renewable power plant's contributions during operation are null. Hourly emissions ($e_{GHG,GT}$), commonly expressed in units of equivalent CO_2 (CO_2eq) for a given period, can be evaluated from P_{fuel} by assuming a typical emission factor per fuel and machine. For example, typical emission factor values are 202 kg/MWh_{fuel} in the case of aero-derivative GTs [43] and 185 kg/MWh_{fuel} in the case of micro GTs powered by NG [72,90].

A4.4 LHI

The safety indicator used, the Levelized inherent Hazard Index, is defined as in Eq. A7 where HHI_k is an index quantifying the risk for humans and associated to the k-th process unit (here a gas turbine), $P_{GT,t}$ is the power output of the GT park at the t-th hour.

$$LHI = \sum_{k=1}^{N_{GT}} HHI_k / \sum_{k=1}^{T} P_{GT,t} = \sum_{k=1}^{N_{GT}} \sum_{i=1}^{N_{LOCs}} (cf_{i,k} \bullet \max_j d_{i,j,k}^2) / \sum_{k=1}^{T} P_{GT,t} \tag{A7}$$

More in details, HHI_k [m^2/y] is used to quantify the risk for the human target associated with the k-th process unit of the plant in terms of potentially damaged area per year [48]. $d_{i,j,k}$ [m] is the damage distance at which human targets undergo lethal effects when the j-th accident scenario happens as a consequence of the i-th release mode from the k-th process unit. $cf_{i,k}$ [1/y] is the Credit Factor assigned to the i-th release mode, representing the credibility of the event leading to the dispersion of hazardous substances. N_{LOCs} represents the possible release modes of the k-th unit. In order to correctly account for the intermittent operation of the turbines, affecting the credibility factors $cf_{i,k}$, which are normally entailing continuous operation during the year [91], in the newly-defined indicator LHI, the $cf_{i,k}$ are evaluated as in Eq. A8: $CF_{i,k}$ is the credit factor taken from specialized literature and referred to full-year operation [91], h_{op} the number of operation hours in the reference year and h_{year} the number of hours in the year.

$$cf_{i,k} = CF_{i,k} \bullet \frac{h_{op,GT}}{h_{year}} \tag{A8}$$

Table A2
Scores and weights assigned for aggregation of indicators based on different perspectives.

Decision-making perspectives	Criteria	Indicators used for the MCDA			
		LEE	***LCOE* and/ or *LVOE***	***LGHG***	***HHI***
		Score 1–5	*Score 1–5*	*Score 1–5*	*Score 1–5*
Individualist	Time	2	3	3	5
	Space	3	4	3	5
	Receptor	2	4	5	5
	Sum	7	11	11	15
	Weight	**0.159**	**0.250**	**0.250**	**0.341**
Egalitarian	Time	5	3	5	1
	Space	5	3	5	1
	Receptor	4	1	5	1
	Sum	14	7	15	3
	Weight	**0.359**	**0.179**	**0.385**	**0.077**
Hierarchist	Time	3.5	3	4	3
	Space	4	3.5	4	3
	Receptor	3	2.5	5	3
	Sum	10.5	10	13	9
	Weight	**0.253**	**0.217**	**0.313**	**0.217**

Normalization and weighing procedures

A5.1 the normalization procedure

Depending on the definition of the absolute metric, the performance improvement leads to the maximization or minimization of the indicator. There follows the necessity to apply the most appropriate normalization approach to correctly obtain the non-dimensional indicator (X_I): Eq. A9 to those indicators that increase their performance by maximizing their values (as *LEE* and *LVOE*), and Eq. A10 to the ones behaving in the opposite way (*LCOE*, *LGHG*, *LHI*).

$$X_I = \frac{I_{act} - I_{min}}{I_{max} - I_{min}} with \begin{cases} X_I = 1 if I_{act} > I_{max} \\ X_I = 0 if I_{act} < I_{min} \end{cases} \tag{A9}$$

$$X_I = \frac{I_{max} - I_{act}}{I_{max} - I_{min}} with \begin{cases} X_I = 1 if I_{act} < I_{min} \\ X_I = 0 if I_{act} > I_{max} \end{cases} \tag{A10}$$

A5.2 The weighing procedure

The common method to extract trade-offs between indicators is the Analytic Hierarchy Process (AHP) method [49] which makes use of pair-wise comparisons to evaluate the performance of the alternatives on indicators (scoring) and indicators among themselves (weighing) [92]. To limit the intrinsic subjectivity of this process, a literature procedure for deriving importance coefficients is used, which bases the elicitation of trade-offs weights on proper criteria (time–space-receptor) along with three decision-makers perspectives (individualist-egalitarian-hierarchist) [93]. Equal weighting is further added to the archetypes of decision-makers.

Before scoring and weighing, the indicators proposed for the assessment are classified in terms of time, space and receptor criteria based on their definition.

Being a measure of resource use, *LEE* is considered important for a long-term perspective and on a global scale since improvements may lead to a better resource utilization and to lower emissions, with reduced costs. The ecosystem is evaluated as the main receptor by this indicator, but also humans may be influenced since resources' use and costs are human-related aspects.

LCOE and *LVOE* exhibit mainly short-term, local/regional and anthropocentric perspectives. However, they can be considered unimportant over time since externalities (e.g. available resources, sociopolitical variations and other local/regional factors) are internalized into the cost/price assessments.

LGHG is considered a very important long-term and global-scale concern, even though its effect may be on the short-term and at local scale based on the incidence of the weather. Thus, it is evaluated as neutral on time and space criteria. Both humans and ecosystems are sensitive receptors.

LHI is an indicator quantifying the likelihood of severe accident scenarios for human targets. It is short-term with respect to the time horizon. Moreover, it is local in terms of space perspective, as it quantifies the inherent hazard within the area containing the chemical plant/facility. This indicator is consistent with respect to association with humans as opposed to the ecosystem.

For each archetype of decision-makers, given scores in a five-level Likert scale are assigned to the indicators based on these three criteria. The overall score to each indicator is estimated as the sum of the scores given with respect to each criterion. The relative importance of the indicators is determined as the ratio of the associated overall score to the sum of overall scores. All values of assigned scores and weights are reported in Table A.2. These weights are used to derive the pair-wise comparison matrix, the evaluation matrix and the trade-off weights among indicators according to the AHP method.

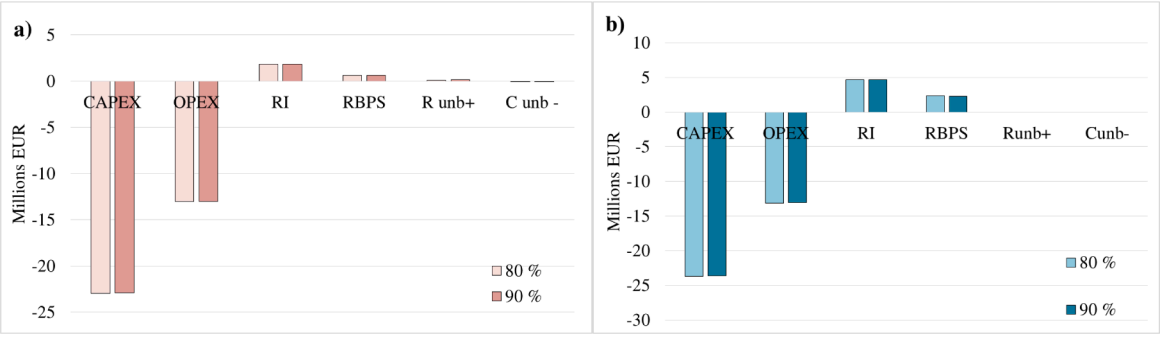

Fig. C1. Costs and revenues obtained in the case of 80% and 90% correct power dispatching in the Adriatic Sea test site (a) and in the North Sea test site (b).

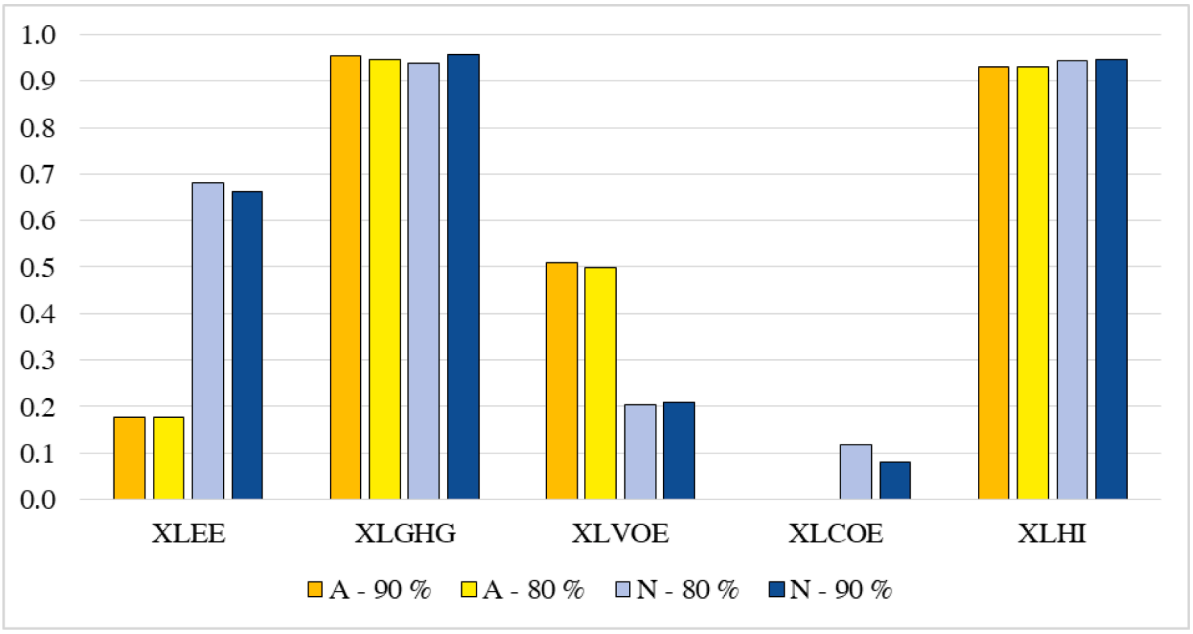

Fig. C2. Normalized metrics compared for the two offshore sites in the case of 80% correct and 90% correct dispatching (A stands for the Adriatic Sea, N for the North Sea).

Appendix B:. Detailed data concerning the sites of the case studies

The site in the Adriatic Sea

The northern area of the Adriatic Sea is characterized by offshore extraction platforms close to decommissioning. Porto Corsini MW C platform was selected (44°51′ N, 12°37′ E) since in 2017 it was harvesting NG from 4 wells out of the 12 originally linked, with an average production of 4960 Sm^3/h and a gas composition mainly consisting of methane after dehydration [58].

From a financial and economic viewpoint, day-ahead prices for the Italian case are retrieved from the site of the Italian body of Electric Market Management "GSE" which provides hourly prices; market data referred to Northern Italy are selected to comply with the hybrid energy plant location [94].

In the Italian case, the participation in the low auction is optimistically supposed to lead to the minimum discount on the base tariff for incentives (2%).

The Italian electricity market also evaluates the positive and negative unbalances by assigning prizes and costs. The allocation of prizes or costs not only depends on the unbalance sign with respect to the dispatch power, but also on the zonal signs and sale/purchase dynamics, which are defined hourly by the national TSO TERNA [33]. Thus, referring to the Northern Italy region and to the reference year 2017, historical hourly data are retrieved from the public dataset "SunSet" where aggregated zonal signs, average sale and purchase prices are available monthly [95].

In the reference year, incentives on RE were regulated by a decree of the Italian Ministry of Economic Development in force since 2016. The decree foresaw indirect access to incentives by means of a low auction on the base tariff (discounted from 2 to 40%) for those hybrid plants whose total capacity fell below the threshold value set for the nominal potential of the sole RE generators; moreover, the produced energy eligible for incentives, defined as the total generation diminished of the thermal energy in input, was to be at least the 5% of the totality. In the case of hybrid energy facilities based on ocean energy, the threshold was 5 MW and the base incentive tariff amounted to 300 EUR/MWh [96].

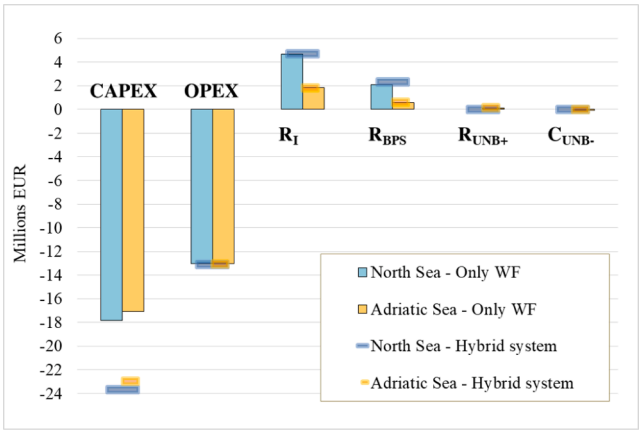

Fig. C3. Costs and revenues obtained in the case of sole wave farms applied in the test-sites, compared with the respective results obtained for scenario A (hybrid systems).

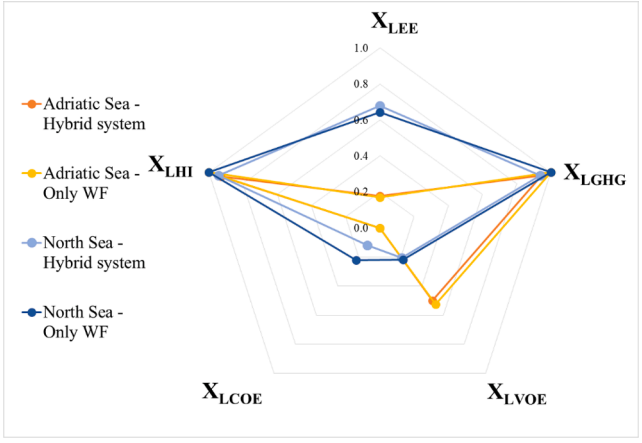

Fig. C4. Normalized sustainability indicators calculated for the two test sites according to the scenario of sole wave farms operating.

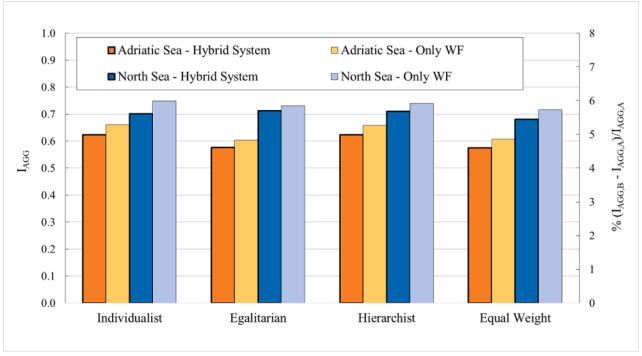

Fig. C5. ASI results according to the four decision-making perspectives: a) scenario A; b) scenario B; c) scenario C.

The site in the North Sea

The North Sea hosts several oil and gas reserves, divided according to blocks as displayed in the Dutch Oil and Gas portal [61]. In the North Sea, the L11 block was considered and well L11B-A-08 was selected out of the two still open in 2017, being the extraction end foreseen for 2018. L11B-A-08 is afferent to the near L08-D gas field, which is a common gas–water charged structure located at 50 km from the shore with a sub-sea extension of 37 km^2 [60].

Regarding economics in the North Sea location, the Dutch electricity market is based on day-ahead prices, available hourly on the website of the European Network of Transmission System Operators for Electricity [97]. Incentive tariffs for Dutch renewable generation are established by the

Table C1
Absolute indicators compared for the two offshore sites in the case of 80% and 90% correct power dispatching.

Indicators		Adriatic Sea		North Sea	
		80%	90%	80%	90%
LEE	%	14	14	53	52
LGHG	kg_{CO2eq}/MWh	48.9	40.5	55.5	39.1
LVOE	*EUR/MWh*	290	296.1	119	121.5
LCOE	*EUR/MWh*	3960	4015	610	627
LHI	m^2/MWh	1.14E-04	1.12E-04	9.03E-05	8.74E-05

Table C2
Technological, economic, environmental and inherent safety performances of the sole wave farms operating in the test cases.

TECHNOLOGICAL PERFORMANCE				
			Adriatic Sea	North Sea
Wave Farm	Available wave energy yearly	*MWh*	1143	8875
	Nominal Power	*MW*	1.92	1.92
	Electrical energy produced yearly	*MWh*	598	3919
	EFLH	*h*	312	2044
	h_{WF}	*h*	1648	6450
	Percentage h_{WF}	–	19%	74%
	Average η in h_{WF}	–	70%	68%
GTs park	Nominal Power	*MW*	0	0
	Electrical energy produced yearly	*MWh*	0	0
	EFLH	*h*	0	0
	h_{GT}	*h*	0	0
	Percentage h_{GT}	–	0%	0%
	Average η in h_{GT}	–	NA	NA
Hybrid System	Nominal Power	*MW*	1.92	1.92
	Electrical energy produced yearly	*MWh*	598	3919
	Thermal Energy input	*MWh*	0	0
	LEE	–	13%	50%

ECONOMIC PERFORMANCE				
			Adriatic Sea	North Sea
Revenues from renewable energy incentives R_I		*EUR*	134,135	344,848
Revenues from sales at base market price R_{BPS}		*EUR*	43,645	155,075
Total from sale $A = R_I + R_{BPS}$		*EUR*	177,779	499,923
Revenues / Costs from unbalances	R_{unb+}	*EUR*	9600	0
	C^-_{unb}	*EUR*	−3389	0
	$B = R_{unb+} + C^-_{unb}$	*EUR*	5210	0
Emissions penalties	C_{GHG}	*EUR*	0	0
Total = A + B-C		*EUR*	182,990	499,923
LVOE		*EUR/MWh*	306	128
LCOE		*EUR/MWh*	3600	563

ENVIRONMENTAL PERFORMANCE			
		Adriatic Sea	North Sea
Total emissions	ton_{CO2eq}	0	0
LGHG	kg_{CO2eq}/MWh	0	0

INHERENT SAFETY PERFORMANCE			
		Adriatic Sea	North Sea
HHI	m^2/y	0	0
LHI	m^2/MWh	0	0

Netherlands Enterprise Agency through "SDE+" incentive schemes, to which plant operators can apply in four rounds. Application for incentives was supposed to be carried out in year 2016, while plant production in 2017. Thus, the reference incentive for free flowing energy and wave energy is 12 EUR/MWh, equal to the 2016 average values [98]. This value has to be diminished by a correction amount determined by the energy prices of the current year, thus to enable a good Dutch market representation, the correction amount was taken from "SDE + 2018" where the provisional one (3.8 EUR/MWh) is quantified from the real 2017 price tenors [99]. Moreover, according to "SDE + 2016", the maximum RE eligible for incentives is equivalent to 3700 full load hours and no prizes are assigned to those generation hours following at least 6 h of null energy supply to the grid.

Appendix C:. Detailed results of the scenarios considered

See Figs C1-C5 and Tables C1 and C2.

Scenario B: Hybrid system with 90% probability of correct dispatching

Fully-renewable generation system: A parallel scenario

The following results derive from the application of the proposed sustainability assessment in the case only the wave farms are the installed systems in the considered test-cases, therefore excluding the possibility of supporting the generation with a compensating back-up system.

References

[1] Our World in Data. Share of electricity production from renewables 2021. https://ourworldindata.org/grapher/share-electricity-renewables?tab=chart&stackMode=absolute&time=earliest..latest&country=~OWID_WRL&region=Europe (accessed February 25, 2021).

[2] Our World in Data. Annual change in renewable energy generation 2021. https://ourworldindata.org/grapher/annual-change-renewables?tab=chart&time=2001..2019&country=~OWID_WRL (accessed February 25, 2021).

[3] IRENA. Renewable Energy Finance Flows 2021. https://www.irena.org/Statistics/View-Data-by-Topic/Finance-and-Investment/Renewable-Energy-Finance-Flows (accessed February 25, 2021).

[4] Department of Social and Economic Affairs of United Nations. The 2030 Agenda for Sustainable Development 2021. https://sdgs.un.org/goals (accessed March 10, 2021).

[5] Boshell F, Roesch R, Salgado A, Hecke J. Unlocking the potential of Ocean Energy: from megawatts to gigawatts. EnergypostEu 2021.

[6] The world Factbook. Field listing - coastline. CIAGov 2021. https://www.cia.gov/the-world-factbook/field/coastline/ (accessed February 20, 2021).

[7] IRENA. Renewable energy employment by country 2021. https://www.irena.org/Statistics/View-Data-by-Topic/Benefits/Renewable-Energy-Employment-by-Country (accessed February 26, 2021).

[8] d'Amore-Domenech R, Leo TJ, Pollet BG. Bulk power transmission at sea: Life cycle cost comparison of electricity and hydrogen as energy vectors. Appl Energy 2021;288:116625. https://doi.org/10.1016/j.apenergy.2021.116625.

[9] Irena. Innovation outlook: Ocean energy technologies. Abu Dhabi 2020.

[10] Trivedi K, Koley S. Performance of a hybrid wave energy converter device consisting of a piezoelectric plate and oscillating water column device placed over an undulated seabed. Appl Energy 2023;333:120627. https://doi.org/10.1016/j.apenergy.2022.120627.

[11] Li Y, Ma X, Tang T, Zha F, Chen Z, Liu H, et al. High-efficient built-in wave energy harvesting technology: from laboratory to open ocean test. Appl Energy 2022;322:119498. https://doi.org/10.1016/j.apenergy.2022.119498.

[12] Chen W, Lu Y, Li S, Gao F. A bio-inspired foldable-wing wave energy converter for ocean robots. Appl Energy 2023;334:120696. https://doi.org/10.1016/j.apenergy.2023.120696.

[13] Foteinis S, Tsoutsos T. Strategies to improve sustainability and offset the initial high capital expenditure of wave energy converters (WECs). Renew Sustain Energy Rev 2017;70:775–85. https://doi.org/10.1016/j.rser.2016.11.258.

[14] Hu J, Zhou B, Vogel C, Liu P, Willden R, Sun K, et al. Optimal design and performance analysis of a hybrid system combing a floating wind platform and wave energy converters. Appl Energy 2020;269:114998. https://doi.org/10.1016/j.apenergy.2020.114998.

[15] Kluger JM, Haji MN, Slocum AH. The power balancing benefits of wave energy converters in offshore wind-wave farms with energy storage. Appl Energy 2023;331. https://doi.org/10.1016/j.apenergy.2022.120389.

[16] Jiang X, Gao D, Hua F, Yang Y, Wang Z. An improved approach to wave energy resource characterization for sea states with multiple wave systems. J Mar Sci Eng 2022;10. https://doi.org/10.3390/jmse10101362.

[17] Coe RG, Ahn S, Neary VS, Kobos PH, Bacelli G. Maybe less is more: considering capacity factor, saturation, variability, and filtering effects of wave energy devices. Appl Energy 2021;291:116763. https://doi.org/10.1016/j.apenergy.2021.116763.

[18] López I, Andreu J, Ceballos S, Martínez De Alegría I, Kortabarria I. Review of wave energy technologies and the necessary power-equipment. Renew Sustain Energy Rev 2013;27:413–34. https://doi.org/10.1016/j.rser.2013.07.009.

[19] Reikard G. Integrating wave energy into the power grid: Simulation and forecasting. Ocean Eng 2013;73:168–78. https://doi.org/10.1016/j.oceaneng.2013.08.005.

[20] Armstrong S, Mollaghan D, Blavette A, O'Sullivan D. An initialisation methodology for ocean energy converter dynamic models in power system simulation tools. Proc Univ Power Eng Conf 2012. https://doi.org/10.1109/UPEC.2012.6398685.

[21] Reikard G, Robertson B, Bidlot JR. Combining wave energy with wind and solar: short-term forecasting. Renew Energy 2015;81:442–56. https://doi.org/10.1016/j.renene.2015.03.032.

[22] Guo Z, Zhang R, Wang L, Zeng S, Li Y. Optimal operation of regional integrated energy system considering demand response. Appl Therm Eng 2021;191:116860. https://doi.org/10.1016/j.applthermaleng.2021.116860.

[23] Capstone Turbine Corporation. C200S ICHP Microturbine. 2021.

[24] du Toit M, Engelbrecht N, Oelofse SP, Bessarabov D. Performance evaluation and emissions reduction of a micro gas turbine via the co-combustion of H2/CH4/CO2 fuel blends. Sustain Energy Technol Assessments 2020;39:100718. https://doi.org/10.1016/j.seta.2020.100718.

[25] Kolian SR, Godec M, Sammarco PW. Alternate uses of retired oil and gas platforms in the Gulf of Mexico. Ocean Coast Manag 2019;167:52–9. https://doi.org/10.1016/j.ocecoaman.2018.10.002.

[26] van Elden S, Meeuwig JJ, Hobbs RJ, Hemmi JM. Offshore Oil and Gas Platforms as Novel Ecosystems: A Global Perspective. Front Mar Sci 2019;6. https://doi.org/10.3389/fmars.2019.00548.

[27] Ou TC, Lu KH, Huang CJ. Improvement of transient stability in a hybrid power multi-system using a designed NIDC (Novel Intelligent Damping Controller). Energies 2017;10. https://doi.org/10.3390/en10040488.

[28] Oliveira-Pinto S, Rosa-Santos P, Taveira-Pinto F. Electricity supply to offshore oil and gas platforms from renewable ocean wave energy: Overview and case study analysis. Energy Convers Manag 2019;186:556–69. https://doi.org/10.1016/j.enconman.2019.02.050.

[29] Dallavalle E, Cipolletta M, Casson Moreno V, Cozzani V, Zanuttigh B. Towards green transition of touristic islands through hybrid renewable energy systems. A case study in Tenerife, Canary Islands. Renew Energy 2021;174:426–43. https://doi.org/10.1016/j.renene.2021.04.044.

[30] Dincer I, Cozzani V, Crivellari A. HYBRID ENERGY SYSTEMS FOR OFFSHORE APPLICATIONS. Joe Hayton: HYbrid Ene; 2021.

[31] Nasrollahi S, Kazemi A, Jahangir M-H, Aryaee S. Selecting suitable wave energy technology for sustainable development, an MCDM approach. Renew Energy 2023;202:756–72. https://doi.org/10.1016/j.renene.2022.11.005.

[32] Jahangir MH, Mazinani M. Evaluation of the convertible offshore wave energy capacity of the southern strip of the Caspian Sea. Renew Energy 2020;152:331–46. https://doi.org/10.1016/j.renene.2020.01.012.

[33] Terna S.p.A. Terna - driving energy 2021. https://www.terna.it/it (accessed May 27, 2021).

[34] Sun P, Xu B, Wang J. Long-term trend analysis and wave energy assessment based on ERA5 wave reanalysis along the Chinese coastline. Appl Energy 2022;324:119709. https://doi.org/10.1016/j.apenergy.2022.119709.

[35] Reikard G, Pinson P, Bidlot JR. Forecasting ocean wave energy: The ECMWF wave model and time series methods. Ocean Eng 2011;38:1089–99. https://doi.org/10.1016/j.oceaneng.2011.04.009.

[36] Fernández-Chozas J, Kofoed JP, Jensen NEH. User guide – COE Calculation tool for Wave Energy Converters ver. 1.6. Allborg - Denmark: 2014.

[37] Babarit A, Hals J, Muliawan MJ, Kurniawan A, Moan T, Krokstad J. Numerical benchmarking study of a selection of wave energy converters. Renew Energy 2012;41:44–63. https://doi.org/10.1016/j.renene.2011.10.002.

[38] de Andres A, Maillet J, Todalshaug JH, Möller P, Bould D, Jeffrey H. Techno-economic related metrics for a wave energy converters feasibility assessment. Sustain 2016:8. https://doi.org/10.3390/su8111109.

[39] O'Connor M, Lewis T, Dalton G. Techno-economic performance of the Pelamis P1 and Wavestar at different ratings and various locations in Europe. Renew Energy 2013;50:889–900. https://doi.org/10.1016/j.renene.2012.08.009.

[40] Vannucchi V, Cappietti L. Wave energy assessment and performance estimation of state of the artwave energy converters in italian hotspots. Sustain 2016:8. https://doi.org/10.3390/su8121300.

[41] Nilsson D, Westin A. Floating wind power in Norway: Analysis of opportunities and challenges 2014.

[42] Wang F, Pei Y, Boroyevich D, Burgos R, Ngo K. Ac vs. dc distribution for off-shore power delivery. IECON Proc (Industrial Electron Conf 2008:2113–8. https://doi.org/10.1109/IECON.2008.4758283.

[43] Guandalini G, Campanari S, Romano MC. Power-to-gas plants and gas turbines for improved wind energy dispatchability: Energy and economic assessment. Appl Energy 2015;147:117–30. https://doi.org/10.1016/j.apenergy.2015.02.055.
[44] Tugnoli A, Landucci G, Salzano E, Cozzani V. Supporting the selection of process and plant design options by Inherent Safety KPIs. J Loss Prev Process Ind 2012;25:830–42. https://doi.org/10.1016/j.jlp.2012.03.008.
[45] Cipolletta M, Moreno VC, Cozzani V. Inherent safety assessment for two solar-based fuels production processes: Methanol via co2 catalytic hydrogenation and biodiesel from microalgal oil. Chem Eng Trans 2020;82:85–90. https://doi.org/10.3303/CET2082015.
[46] Crivellari A, Bonvicini S, Tugnoli A, Cozzani V. Multi-target Inherent Safety Indices for the Early Design of Offshore Oil&Gas Facilities. Process Saf Environ Prot 2021;148:256–72. https://doi.org/10.1016/j.psep.2020.10.010.
[47] IEA, NEA. Projected Costs of Generating Electricity 2015:1–215.
[48] Crivellari A, Tugnoli A, Cozzani V, Macini P. Systematic methodology for inherent safety indicators assessment of early design stages of offshore oil & gas projects. Chem Eng Sci 2018;67:691–6. https://doi.org/10.3303/CET1867116.
[49] Saaty TL. The analytic hierarchy process. New York: McGraw-Hill International Book Co; 1980.
[50] Silva D, Rusu E, Soares CG. Evaluation of various technologies for wave energy conversion in the portuguese nearshore. Energies 2013;6:1344–64. https://doi.org/10.3390/en6031344.
[51] OECD. Renewable energy feed-in tariffs. OECDStats 2020. https://stats.oecd.org/Index.aspx?DataSetCode=RE_FIT (accessed February 16, 2020).
[52] European Environment Agency. Greenhouse gas emission intensity of electricity generation in Europe 2020. https://www.eea.europa.eu/data-and-maps/indicators/overview-of-the-electricity-production-3/assessment (accessed February 17, 2020).
[53] Metropolis N, Ulam S. The Monte Carlo Method. J Am Stat Assoc 1949;44:335–41.
[54] Dialyna E, Tsoutsos T. Wave energy in the mediterranean sea: Resource assessment, deployed wecs and prospects. Energies 2021:14. https://doi.org/10.3390/en14164764.
[55] Mørk G, Barstow S, Kabuth A, Pontes MT. Assessing the global wave energy potential. Proc Int Conf Offshore Mech Arct Eng - OMAE 2010;3:447–54. https://doi.org/10.1115/OMAE2010-20473.
[56] ARPAE. DEXT3R 2021. https://simc.arpae.it/dext3r/ (accessed May 27, 2021).
[57] EMODnet physics. ERDAPP 2021. https://erddap.emodnet-physics.eu/erddap/index.html (accessed May 8, 2021).
[58] Gamna V. Eni apre le porte della piattaforma Garibaldi C. AffariitalianiIt 2019:5.
[59] Ministero dello Sviluppo Economico. Piattaforme e teste pozzo sottomarine. 2020.
[60] Offshore Technology. L8-D field, North Sea 2010. https://www.offshore-technology.com/projects/l8dfieldnorthsea/ (accessed September 15, 2020).
[61] NLOG. Dutch Oil and Gas portal 2021. https://www.nlog.nl/en/map-boreholes (accessed November 10, 2020).
[62] Marine Traffic. Platform L11-B 2021. https://www.marinetraffic.com/no/ais/details/ships/shipid:4795744/mmsi:245651000/imo:0/vessel:PLATFORM_L11B (accessed July 12, 2020).
[63] Lira-Loarca A, Ferrari F, Mazzino A, Besio G. Future wind and wave energy resources and exploitability in the Mediterranean Sea by 2100. Appl Energy 2021;302:117492. https://doi.org/10.1016/j.apenergy.2021.117492.
[64] Sørensen HC, Friis-Madsen E. Wave Dragon 1.5 MW North Sea Demonstrator - Phase 1. 2015.
[65] Hong Y, Eriksson M, Boström C, Waters R. Impact of generator stroke length on energy production for a direct drivewave energy converter. Energies 2016;9. https://doi.org/10.3390/en9090730.
[66] Miguel Sagaseta de Ilurdoz Cortadellas A, Miguel Ángel Guerra Rodríguez B, Raquel Ramos Pereda C, Cuesta Moreno DPD. Preliminary study for the implementation of the “wave dragon” in Gran Canaria, Canary Islands, Spain. Renew Energy Power Qual J 2011;1:1111–6. https://doi.org/10.24084/repqj09.560.
[67] Pecher A. Performance Evaluation of Wave Energy Converters. 2013. https://doi.org/10.13052/rp-9788792982278.
[68] Sørensen HC, Friis-Madsen E. Wave Dragon 1.5 MW North Sea Demonstrator - Phase 1 2014:2012–4.
[69] U.S. DOE. Combined Heat and Power Technology Fact Sheet Series: Microturbines. 2016.
[70] European Commission. EU ETS Handbook. Clim Action 2015:138.
[71] de Andres A, Guanche R, Vidal C, Losada IJ. Adaptability of a generic wave energy converter to different climate conditions. Renew Energy 2015;78:322–33. https://doi.org/10.1016/j.renene.2015.01.020.
[72] U.S. Department of Energy. Combined Heat and Power Technology Fact Sheet Series - Microturbines 2016:1–4. https://doi.org/DOE/EE-1329.
[73] Reikard G, Robertson B, Bidlot JR. Wave energy worldwide: simulating wave farms, forecasting, and calculating reserves. Int J Mar Energy 2017;17:156–85. https://doi.org/10.1016/j.ijome.2017.01.004.
[74] Ackermann T. Wind Power in Power Systems. John Wiley & Sons, Ltd; 2005. https://doi.org/10.1002/0470012684.
[75] Pinson P, Reikard G, Bidlot JR. Probabilistic forecasting of the wave energy flux. Appl Energy 2012;93:364–70. https://doi.org/10.1016/j.apenergy.2011.12.040.
[76] Penalba M, Ringwood JV. A review of wave-to-wire models for wave energy converters. Energies 2016;9. https://doi.org/10.3390/en9070506.
[77] Hughes SA. Advanced Series on Ocean Engineering: Volume 7 - Physical Models and Laboratory Techniques in Coastal Engineering. World Scientific Publishing Co Pte Ltd; 1993. https://doi.org/10.1142/asoe10.1142/2154.
[78] Capstone Turbine Corporation. Capstone microturbines 2019.
[79] do Nascimento MAR, Rodrigues LDO, E. C. Dos Santos EEBG, Dias FLG, Velásques EIG, Carrillo R a. M. Micro Gas Turbine Engine: A Review 2014:107–42. https://doi.org/10.5772/54444 13.
[80] Barelli L, Ottaviano A. Supercharged gas turbine combined cycle: An improvement in plant flexibility and efficiency. Energy 2015;81:615–26. https://doi.org/10.1016/j.energy.2015.01.004.
[81] Liu Z, Karimi IA. Simulation and optimization of a combined cycle gas turbine power plant under part-load operation. Comput Aided Chem Eng 2018;44:2401–6. https://doi.org/10.1016/B978-0-444-64241-7.50395-5.
[82] Trapani K, Millar DL. Proposing offshore photovoltaic (PV) technology to the energy mix of the Maltese islands. Energy Convers Manag 2013;67:18–26. https://doi.org/10.1016/j.enconman.2012.10.022.
[83] Kim TS. Comparative analysis on the part load performance of combined cycle plants considering design performance and power control strategy. Energy 2004;29:71–85. https://doi.org/10.1016/S0360-5442(03)00157-9.
[84] Li Y, Zhang G, Bai Z, Song X, Wang L, Yang Y. Backpressure adjustable gas turbine cycle: a method to improve part-load efficiency. Energy Convers Manage 2018;174:739–54. https://doi.org/10.1016/j.enconman.2018.07.077.
[85] Boyce MP. An Overview of Gas Turbines. Gas Turbine Eng. Handb. 4th ed., Oxford, United Kingdom: Butterworth-Heinemann Elsevier Inc.; 2012. https://doi.org/10.1016/C2009-0-64242-2.
[86] U.S. DOE. CHP Technology Factsheet Series: Gas Turbine 2016:4.
[87] U.S. Department of Energy. Combined Heat and Power Technology Factsheet Series: Gas Turbines 2016:1–4.
[88] World Bank Group. Report of the High-Level Commission on Carbon Prices 2017:1–69.
[89] World Bank, Ecofys. State and Trends of Carbon Pricing 2018. Washington DC, USA: International Bank for Reconstruction and Development - The World Bank; 2018. https://doi.org/10.1596/978-1-4648-1292-7.
[90] U.S. Environmental Protection Agency. Greenhouse Gas (GHG) Verification Guideline Series: Natural Gas-Fired Microturbine Electrical Generators 2002.
[91] Uijt de Haag PAM, Ale BJM. The “Purple book” – Guidelines for quantitative risk assessment. Publ Ser Danger Subst (PGS 3) 2005:237.
[92] Belton V, Stewart T. Multiple criteria decision analysis: an integrated approach. Boston: Kluwer Academic Publishers; 2002.
[93] Hacatoglu KA. Systems Approach to Assessing the Sustainability of Hybrid Community Energy Systems. University of Ontario Institute of Technology; 2014.
[94] GSE. Esiti MGP - prezzi 2021. https://mercatoelettrico.org/It/Esiti/MGP/EsitiMGP.aspx (accessed May 27, 2021).
[95] SunSet. Storico segno giornaliero. MyTerna 2021. https://myterna.terna.it/SunSet/Public/Pubblicazioni (accessed May 27, 2021).
[96] Ministero dello Sviluppo Economico. Ministerial Decree 23 June 2016. Incentive for electric energy produced from renewable sources apart from PV. 2016.
[97] ENTSO-E. Day-ahead prices. Eur Netw Transm Syst Oper Electr 2021. https://transparency.entsoe.eu/transmission-domain/r2/dayAheadPrices (accessed May 27, 2021).
[98] Netherlands Enterprise Agency. SDE+ 2016. 2016.
[99] Netherlands Enterprise Agency. SDE+ Spring 2018. 2018.